Title

Novel mutations in BRCA2 intron 11 and overexpression of COX-2 and BIRC3 mediate cellular resistance to PARP inhibitors.

Journal

American Journal of Cancer Research, 10(9)

ISSN

2156-6976

Authors

Chen, Hua-Dong
Guo, Ne
Song, Shan-Shan
et al.

Publication Date

2020

Peer reviewed

Am J Cancer Res 2020;10(9):2813-2831
www.ajcr.us /ISSN:2156-6976/ajcr0116181

Original Article

Novel mutations in *BRCA2* intron 11 and overexpression of COX-2 and BIRC3 mediate cellular resistance to PARP inhibitors

Hua-Dong Chen[1,2], Ne Guo[1,2], Shan-Shan Song[1,2], Chuan-Huizi Chen[1,2], Ze-Hong Miao[1,2,3], Jin-Xue He[1,2]

[1]Division of Anti-Tumor Pharmacology, State Key Laboratory of Drug Research, Shanghai Institute of Materia Medica, Chinese Academy of Sciences, Shanghai 201203, P. R. China; [2]University of Chinese Academy of Sciences, No. 19A Yuquan Road, Beijing 100049, P. R. China; [3]Open Studio for Drugability Research of Marine Natural Products, Pilot National Laboratory for Marine Science and Technology (Qingdao), 1 Wenhai Road, Aoshanwei, Jimo, Qingdao 266237, Shandong, P. R. China

Received June 12, 2020; Accepted July 23, 2020; Epub September 1, 2020; Published September 15, 2020

Abstract: Several poly(ADP ribose) polymerase (PARP) inhibitors (PARPi) have been approved for cancer therapy; however, intrinsic and acquired resistance has limited their efficacy in the clinic. In fact, cancer cells have developed multiple mechanisms to overcome PARPi cytotoxicity in even a single cancer cell. In this study, we generated three PARPi-resistant BRCA2-deficient pancreatic Capan-1 variant cells using olaparib (Capan-1/OP), talazoparib (Capan-1/TP), and simmiparib (Capan-1/SP). We identified novel mutations in intron 11 of *BRCA2*, which resulted in the expression of truncated BRCA2 splice isoforms. Functional studies revealed that only a fraction (32-49%) of PARPi sensitivity could be rescued by depletion of BRCA2 isoforms. In addition, the apoptosis signals (phosphatidylserine eversion, caspase 3/7/8/9 activation, and mitochondrial membrane potential loss) were almost completely abrogated in all PARPi-resistant variants. Consistently, overexpression of the anti-apoptotic proteins cyclooxygenase 2 (COX-2) and baculoviral IAP repeat-containing 3 (BIRC3) occurred in these variants. Depletion of COX-2 or BIRC3 significantly reduced apoptotic resistance in the PARPi-resistant sublines and reversed PARPi resistance by up to 70-72%. Furthermore, exogenous addition of prostaglandin E2, a major metabolic product of COX-2, inhibited PARPi-induced apoptotic signals; however, when combined with the BIRC3 inhibitor LCL161, there was significantly enhanced sensitivity of the resistant variants to PARPi. Finally, PARPi treatment or PARP1 depletion led to a marked increase in the mRNA and protein levels of COX-2 and BIRC3, indicating that PARP1 is a negative transcriptional regulator of these proteins. Together, our findings demonstrated that during the chronic treatment of cells with a PARPi, both *BRCA2* intron 11 mutations and COX-2/BIRC3-mediated apoptotic resistance led to PARPi resistance in pancreatic Capan-1 cells.

Keywords: PARP inhibitors resistance, BRCA2, COX-2, BIRC3, apoptotic resistance

Introduction

Poly(ADP ribose) polymerase (PARP) inhibitors (PARPi) are primarily used as a monotherapy to treat homologous recombination repair (HRR)-deficient cancers. Currently, four different PARPi have been approved for the treatment of ovarian and breast cancers [1-5], and more are being tested in clinical trials [1, 6, 7]. However, the emergence of acquired resistance to PARPi has followed the introduction of therapeutics in the clinic [8-10]. Several mechanisms of PARPi resistance have been identified including restoration of homologous recombination repair (HRR) activity due to secondary mutation of *BRCA1/2* genes or depletion of the 53BP1-RIF1-REV7 pathway, loss of PAR glycohydrolase (PARG) or the drug target PARP1, and upregulation of P-glycoprotein (P-gp) [1].

HRR restoration has been observed in BRCA2-deficient pancreatic cancer Capan-1 cells that have re-established BRCA2 function. Novel BRCA2 isoforms with partial function are expressed in PARPi-resistant cells as the result of secondary revertant mutations of the *BRCA2*

gene and restoration of open reading frames (ORFs) [11, 12]. However, secondary *BRCA2* mutations explain only some of the cases of PARPi resistance. Moreover, a number of reports have shown that resistant cells have BRCA2 gene mutation without restoration of HRR function [13-18]. Furthermore, in the absence of BRCA1, HRR activity can be bypassed by loss of 53BP1 or REV7 [19, 20]. In contrast, there is no evidence that HRR can be rescued in the absence of BRCA2, suggesting that BRCA2-deficient cancer cells may employ a novel strategy to overcome PARPi cytotoxicity. To date, there is only limited information on HRR-independent mechanisms of PARPi resistance. Therefore, many issues on drug resistance to PARPi remain to be clarified.

Previous studies have shown that PARP inhibition causes DNA double-strand break (DSB) accumulation and thus G2/M arrest, apoptosis, and subsequent cell death in HRR-deficient cells [6, 7, 21-23]. Activation of caspases 3, 7, and 9 was induced in concentration- and time-dependent manners by PARPi, and pretreatment with the cell-permeable pan-caspase inhibitor Z-VAD-FMK significantly reversed these effects, suggesting that the caspase-dependent apoptotic pathway plays a critical role in the antitumor efficiency of PARPi [6, 7, 21]. Tumor cells can acquire resistance to chemotherapy and immunotherapy by overexpression of the inhibitor of apoptosis protein (IAP) family of proteins (cIAP1/BIRC2, cIAP2/BIRC3) to counteract apoptosis [24-26]. Overexpression of cyclooxygenase 2 (COX-2) in a variety of cancer cells is associated with apoptotic resistance and is thought to be responsible for resistance to chemotherapy and radiation [27]. Thus, there is no doubt that acquired apoptotic resistance plays an important role in promoting drug resistance. However, there have been no reports on the relationship between apoptosis and resistance to PARPi.

Cancer cells employ multiple mechanisms, including HRR-dependent and HRR-independent pathways, to overcome cytotoxicity caused by PARP inhibition. To understand the mechanisms of resistance to PARPi in BRCA2 mutation cancer, we generated a series of PARPi-resistant cells by separately exposing pancreatic cancer Capan-1 cells to olaparib (OP), simmiparib (SP), and talazoparib (TP), and obtained three PARPi resistance variants denoted as Capan-1/OP, Capan-1/SP, and Capan-1/TP, respectively. We demonstrated that Capan-1 cells conferred novel mutations in intron 11 of *BRCA2* and highly expressed COX-2 and BIRC3 to develop cellular resistance to PARPi.

Materials and methods

Antibodies and chemicals

Antibodies against PARP1 (sc-7150), Histone H3 (sc-8654-R), P-gp (sc-13131), PTIP (sc-367459), Chk1 (sc-8408), γH2AX (sc-101696), p-ATM-Ser1981 (sc-47739), DNA-PKcs (sc-9051), β-Actin (sc-47778) and Rad51 (sc-8349) were from Santa Cruz Biotechnology (Santa Cruz, CA). Antibodies against KU80 (#2753), NF-κB p65 (#4764), SMC1 (#4802), ATR (#13934), p-Chk1-Ser345 (#2348), Caspase 3 (#9662), Caspase 9 (#95022), COX-2 (#12282), BIRC3 (#3130), and C-BRCA2 (#10741) were from Cell Signaling Technology (Danvers, MA). Antibodies against PARP2 (ab176330), BCRP (ab3380), and N-BRCA2 (ab123491) were from Abcam (Shanghai, China). The anti-PARP3 antibody (NBP2-49523) was from Novus (Novus Biologicals, CO, USA). The anti-PAR polyclonal antibody (4336-BPC-100) was from Trevigen (Gaithersburg, MD). The anti-REV7 antibody (612266) was from BD Biosciences (Franklin Lakes, NJ). Anti-GAPDH mouse monoclonal antibodies (AG019) were purchased from Beyotime (Shanghai, China). The secondary antibodies used for used for Western blotting included HRP-conjugated goat anti-rabbit and goat anti-mouse antibodies (Jackson ImmunoResearch Laboratories, Inc., West Grove, PA, USA), and those for indirect immunofluorescence were goat anti-mouse Alexa 488 and anti-rabbit Alexa 594 (A21121 and A11012; Invitrogen, Carlsbad, CA, USA).

Olaparib was purchased from LC Laboratories (Woburn, MA, USA), and Simmiparib was provided by Dr. Ao Zhang at Shanghai Institute of *Materia Medica*, Chinese Academy of Sciences, Shanghai, China and prepared as previously described [7, 28]. Talazoparib, niraparib, rucaparib and prostaglandin E2 (PGE2) were purchased from Selleck Chemicals (Shanghai, China). SN38 was purchased from Melone Pharmaceutical (Dalian, China). LCL161 was purchased from MedChemExpress (Shanghai, China). All of the drugs were dissolved in 100%

dimethyl sulfoxide (DMSO), aliquoted, and stored at -20°C. Upon use, inhibitors were diluted to the desired concentration in normal saline to a final DMSO concentration not exceeding 0.1%. Of note, 1‰ and 0.5‰ methyl methane sulfonate (MMS) were freshly prepared each time from 99% MMS (Sigma-Aldrich; St. Louis, MO, USA) in normal saline, and then diluted in complete culture medium to the desired final concentration.

Cell culture

Human Capan-1, BxPC-3, SKOV-3, and RD-ES cells were purchased from the American Type Culture Collection (Manassas, VA, USA). U251 cells were purchased from the Institute of Cell Biology (Shanghai, China). A vincristine-selected resistant KB/VCR subline and KB cells was from the Sun Yat-sen University of Medical Sciences (Guangzhou, China). All of the cells were cultured according to the suppliers' instructions.

Establishment of PARPi-resistant variants

PARPi-resistant variants from pancreatic cancer Capan-1 cells were generated by treating parental cells with increasing concentrations of PARPi as described in the results section. PARPi-resistant variants U251/OP from glioblastoma U251 cells were obtained from our laboratory [29]. PARPi simmiparib-resistant variants RD-ES/SP from Ewing's sarcoma RD-ES cells were obtained in same way [29], specifically by the concentrations of PARPi simmiparib were increased stepwise from 0.1 μM to 5 μM for 84 days.

Cell viability assays

Cells were exposed to gradient concentrations of PARPi for 7 days. Cell viability was assessed using Sulforhodamine B (SRB) assays or CCK-8 assays and recorded with the Spectra-MAX190 Microplate Reader (Molecular Devices, San Jose, CA, USA) as previously described [30, 31]. The averaged IC_{50} values were determined with the Logit method from three independent experiments.

Western blotting

Cells were treated with the indicated drugs for the indicated times. Western blotting was used to measure the cellular levels of the indicated proteins, as previously described [7]. A Subcellular Protein Fractionation Kit (#78840; Thermo Fisher Scientific, Waltham, MA, USA) was used to separate and obtain the chromatin fraction according to the manufacturer's instructions for PARP1-DNA trapping assays [7].

Intracellular PAR formation assays

Intracellular PAR formation and inhibition were analyzed using the In-Cell Analyzer 2000 (GE Healthcare, Waukesha, WI, USA) as previously described [31].

Immunofluorescence assays

Cells were seeded onto glass coverslips, cultured overnight, and treated with PARPi or irradiated (6 Gy) for the indicated times. The treated cells were fixed in pre-cooled methanol at -20°C for 20 min, blocked in 3% bovine serum albumin for 15 min, incubated with primary antibodies for 1 h, and then incubated with fluorescence-conjugated secondary antibodies for 30 min. Finally, the cells were counterstained with DAPI and imaged with an Olympus confocal microscope (Olympus, Tokyo, Japan) at 100 × optical magnification. The percentage of Rad51 or phosphorylated H2AX (γH2AX) or phosphorylated ataxia telangiectasia mutated (p-ATM) foci-positive cells (>3 foci in one cell) was calculated based on the analysis of randomly chosen fields that included at least 200 cells.

DNA sequencing

Total RNA was prepared with TRIzol reagent (Invitrogen) and reverse-transcribed into cDNA with the PrimeScript RT Reagent Kit (TaKaRa, Tokyo, Japan). Genomic DNA was collected using a Genomic DNA Miniprep Kit (Corning, NY, USA). PCR reactions for amplification of *BRCA2* cDNA and genomic fragments were performed with KOD Plus DNA Polymerase (TOYOBO, Tokyo, Japan). Then the amplification products were sequenced by Majorbio Pharmaceutical Technology Co., Ltd. (Shanghai, China). The *BRCA2* primer sequences were as follows: B2CDS11-F: 5'-AGCACGCATTCACATAAGGTT-3'; B2Ex13R1: 5'-GATTACCTGTGTACCCTTTCG-3'; B2CDS11-F: 5'-AGCACGCATTCACATAAGGTT-3'; B2Ex12R1: 5'-GGCTTCAAAAAGCACTCCAGA-3'; B2Ex11F1: 5'-CAAGGTACTAGTG-

AAATCACC-3'; B2Ex27R1: 5'-TGAAATGCCTTC-TGTGCAGCC-3'; B2Ex11F2: 5'-CAGACTTCATTA-CTTGAAGC-3'; B2Ex27R2: 5'-CTACTCAAGAAA-TCCAAGGC-3'; B2Ex11F1: 5'-CAAGGTACTAGT-GAAATCACC-3'; B2Ex24R1: 5'-CAAGATGGCT-GAAAGTCTGG-3'; B2Ex11F3: 5'-CTGCCCCAAA-GTGTAAAGAAA-3'; B2Ex24R2: 5'-AATTTGCTG-AAGTGAAGGG-3'; B2Ex11F4: 5'-ATGCAGCCAT-TAAATTGTCC-3'; B2Ex11R1: 5'-CTGTCAGTTCA-TCATCTTCC-3'; B2Ex11F5: 5'-AACCCAGAGCAC-TGTGTAAACT-3'; and B2IN11R1: 5'-AAACCAT-ACTCCCCCAAACTGA-3'.

Sequencing of *ATM*, *BRCA1*, *BRCA2*, *PTEN*, and *TP53* genes with array-based sequence capture and next-generation sequencing was performed by BGI Diagnosis Technology Co., Ltd. (Shenzhen, Guangdong, China).

RNA interference

Knockout of specific genes was accomplished by RNA interference using small interfering RNA (siRNA). The following target sequences were synthesized by GenePharma Co., Ltd. (Shanghai, China): 5'-UUCUCCGAACGUGUCA-CGU-3' for scrambled siRNA (siNC); 5'-CAA-CAATTACGAACCAAACTT-3' for N-BRCA2 (CDS2); 5'-GAAACGGACUUGCUAUUUA-3' for C10-BR-CA2 (CDS10); 5'-GGGCCGUACACUGCUCAAATT-3' for C-BRCA2-1 (CDS25); 5'-GCCUUGGAUUU-CUUGAGUATT-3' for C-BRCA2-2 (CDS26); 5'-GC-AGCUUCCUGAUUCAAAUTT-3' for COX-2-1; 5'-GCUGUCCCUUUACUUCAUUTT-3' for COX-2-2; 5'-GCAGAUUCGUUCAGAGUCUTT-3' for BIRC3-1; and 5'-GCCUUGAUGAGAAGUUCCUTT-3' for BIRC3-2.

siRNA transfection was performed with RNA-iMAX Transfection Reagent (Invitrogen) according to the manufacturer's instructions.

Two-tailed comet assays

Cells were treated with the indicated drugs for the indicated time. The two-tailed comet assay was performed as previously described [32].

Trypan blue staining

To estimate the percentage of dead cells, cells were re-suspended in phosphate-buffered saline (PBS), washed twice, and stained with 0.4% trypan blue in PBS. After a 10 min incubation, cells were analyzed using the Countess™ II FL Automated Cell Counter (Thermo Fisher Scientific).

CellTiter-Glo luminescent cell viability assays

Cells (8×10^3 cells in 100 μL/well) were seeded on 96-well plates. After being incubated for 24 h at 37°C, 100 μL of the CTG reagent (CellTiter-Glo®, Promega, USA) was added to each well. The luminescence signal was recorded using the EnVision® Multilabel Reader (PerkinElmer).

Quantitative PCR

Total RNA was prepared with TRIzol reagent (Invitrogen) and reverse-transcribed into cDNA with the PrimeScript RT Reagent Kit (TaKaRa). Then it was amplified with the SYBR Premix EX TaqII Kit (TaKaRa) in the 7500 Fast Real-Time PCR System (Applied Biosystems, Foster City, CA, USA). The primers were from Sangon Biotech (Shanghai, China) with the following sequences: COX-2-F: 5'-CAGCAAATCCTTGCTG-TTCCC-3'; COX-2-R: 5'-TGTAGTGCACTGTGTTTG-GAGT-3'; BIRC3-F: 5'-CGCTTTAAAACATTCTTT-AACTGGC-3'; BIRC3-R: 5'-TCTTATCAAGTACTC-ACACCTTGGA-3'; β-actin-F: 5'-GCTGTCTTGGGT-GCATTGGA-3'; and β-actin-R: 5'-AAGGGACTT-CCTGTAACAATGCA-3'.

Mitochondrial membrane potential detection

Cells were treated with the indicated drugs for the indicated times. Then the cells were harvested, washed, and stained using the JC-1 kit (Beyotime, Shanghai, China). The mitochondrial membrane potential (MMP) was analyzed with the FACSCalibur flow cytometer (BD Biosciences, Franklin Lakes, NJ, USA).

Flow cytometry

Cell cycle and apoptosis assays were analyzed by propidium iodide staining-based flow cytometry and Annexin V-FITC apoptosis detection-based flow cytometry as previously described [7]. The data were analyzed with FlowJo software.

Terminal deoxynucleotidyl transferase dUTP nick end labeling assays

Cells were treated with the indicated drugs for the indicated times. The terminal deoxynucleotidyl transferase dUTP nick end labeling (TUNEL) assay was performed with the One Step TUN-

EL Apoptosis Assay Kit (Beyotime, Shanghai, China) according to the manufacturer's instructions.

Caspase activity assays

To assay caspase activity, cells were seeded into 96-well plates (5000 cells in 100 μL per well), cultured overnight, and then treated with the indicated concentrations of drugs for 24-72 h. Activity of caspases 8, 9, and 3/7 in the treated cells was measured using the Caspase-Glo® 8 Assay, Caspase-Glo® 9 Assay, and Caspase-Glo® 3/7 Assay kits (Promega, Fitchburg, WI, USA) according to the manufacturer's instructions. The luminescence value of each sample was measured with the EnVision® Multilabel Reader (PerkinElmer, Waltham, MA, USA).

RealTime-Glo™ Annexin V apoptosis assays

Cells were seeded into 96-well plates (5000 cells in 100 μL per well), cultured overnight, and then treated with the indicated concentrations of drugs for 24-72 h. Exposure of phosphatidylserine (PS) on the outer leaflet of the cell membrane during the apoptotic process was measured using the RealTime-Glo™ Annexin V Apoptosis Assay Kit (Promega) according to the manufacturer's instructions. The luminescence value signal of each sample was measured with the EnVision® Multilabel Reader (PerkinElmer).

Stable knockout of BRCA2 or PARP1 with the CRISPR/Cas9 technique

Lentiviral transfection of cultured cells with pLentiCRISPRv2 vectors encoding *BRCA2* or *PARP1*-specific CRISPR or control vectors (OBIO Technology, Shanghai, China) were performed according to the supplier's instructions. The oligonucleotide single guide RNA sequence for BRCA2 was 5'-ACCGtttacaggagattggtacag-3', and for PARP1 was 5'-CACCGcttgggaccgggatttcatc-3'. Transduced Capan-1 cells were selected with 1 μg/mL puromycin for 2 weeks and downregulated BRCA2 or PARP1 expression was identified by Western blot analysis.

Plasmid and lentivirus infection

The plasmid pLenti-EF1a-EGFP-P2A-Puro-CMV-MCS and lentiviral packaging plasmids were obtained from (OBIO Technology, Shanghai, China). Briefly, COX-2 expression plasmid was created by ligating the full-length coding region of human *PTGS2* into the vector; then lentiviruses were packaged in 293T cells co-transfected with a plasmid with or without *PTGS2* and a cocktail of the packaging plasmids pGAG, pREV and pVSVG. Lentiviral infection was performed at approximately multiplicity of infection (MOI) = 5.

Statistical analyses

All of the data, if applicable, were presented as the mean ± standard deviation (SD). Comparison between two groups was performed with the Student's *t* test. *P* values less than 0.05 were considered to be statistically significant.

Results

Establishment of PARPi-resistant variants from pancreatic cancer Capan-1 cells

To investigate the molecular mechanisms underlying the acquired resistance to PARPi, the pancreatic cancer Capan-1 cells, which harbor the truncated protein c.6174delT frameshift mutation of BRCA2, were separately exposed to increasing concentrations of simmiparib, olaparib and talazoparib. As shown in **Figure 1A**, the concentrations of simmiparib, olaparib, and talazoparib were increased stepwise from 0.5 μM to 5 μM, 1 μM to 60 μM, and 0.025 μM to 0.5 μM, respectively. After exposure of cells to simmiparib, olaparib, and talazoparib for 136, 246, and 169 days, respectively, cells were subcloned, and three PARPi-resistant variants were obtained that were denoted as Capan-1/SP, Capan-1/OP, and Capan-1/TP (**Figure 1A**). The resistant variants acquired 1916-, 46-, and 70-fold resistance to the corresponding PARPi, respectively (**Figures 1B**, **1C** and S1A). Moreover, all three variants showed cross-resistance to other PARPi, including olaparib, simmiparib, talazoparib, rucaparib and niraparib, with resistance factor ranges of 12-46, 789-1921, 71-118, 8-9, and 7-10, respectively (**Figure 1D**). Notably, the resistance of these resistant variants was much higher to simmiparib and talazoparib than olaparib, niraparib and rucaparib. Resistance to the PARPi did not significantly change after 1 year of drug withdrawal, indicating that the

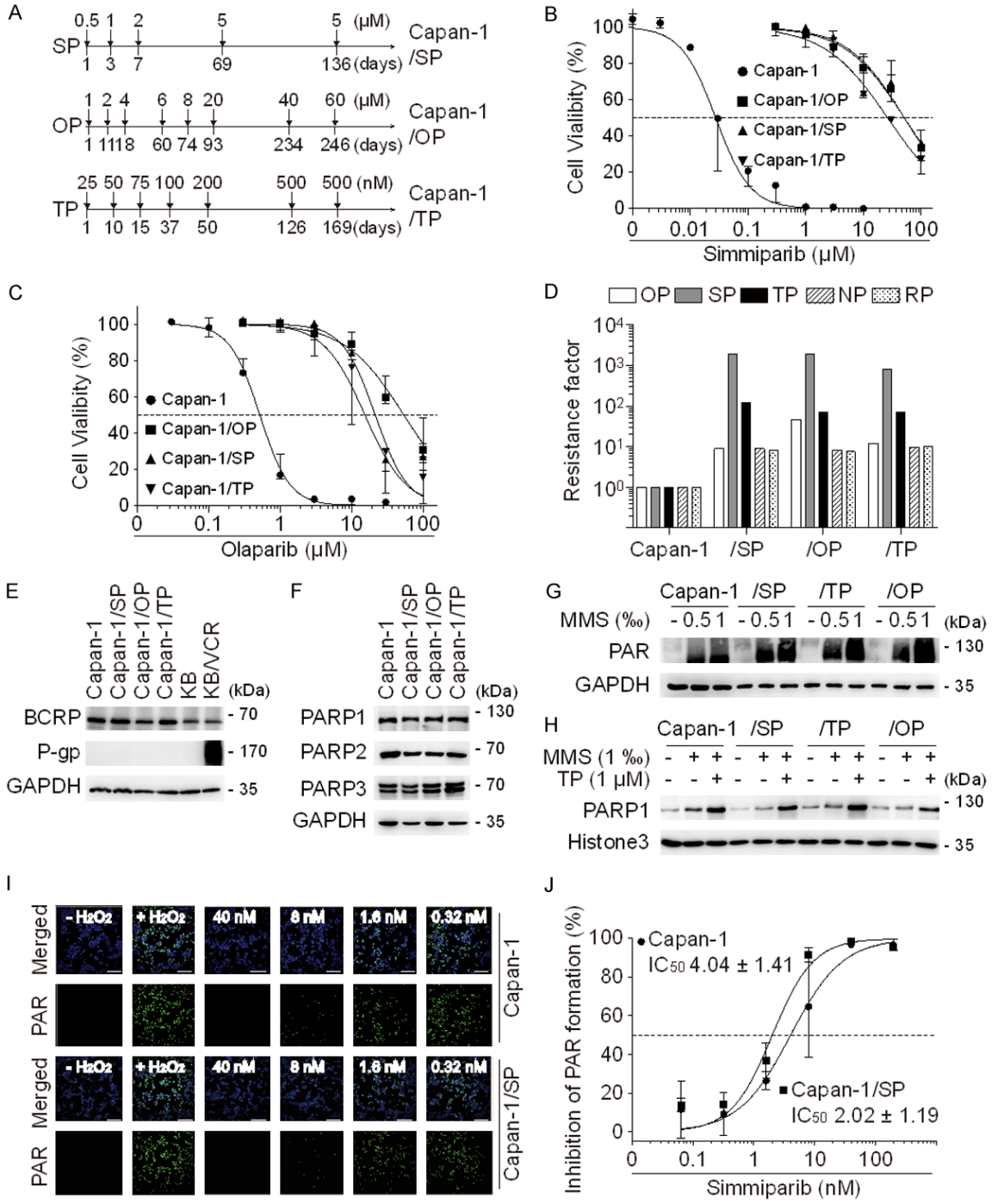

Figure 1. BRCA2-deficient Capan-1 cells develop drug resistance to PARPi, independent of PARP activation and PARP1-DNA trapping. (A) Schematic representation of the generation of PARPi-resistant cells. BRCA2-deficient pancreatic cancer Capan-1 cells were separately exposed to increasing concentrations of simmiparib (SP), olaparib (OP) and talazoparib (TP), and the resistant monoclones were denoted Capan-1/SP (/SP), Capan-1/OP (/OP), and Capan-1/TP (/TP), respectively. (B and C) Cells were treated with simmiparib (B) or olaparib (C) for 7 days and subjected to SRB assays. (D) Cross-resistance of PARPi-resistant variants. Cells were exposed to olaparib (OP), talazoparib (TP), simmiparib (SP), niraparib (NP) or rucaparib (RP) for 7 days and assessed by SRB assays. The resistance factor was calculated as the ratio of the averaged IC_{50} value of the indicated PARPi in the given resistant cells to that of the same PARPi in the parental Capan-1 cells. (E and F) Protein levels of the drug transporters P-gp, BCRP (E) and PARP1, PARP2, PARP3 (F) detected by Western blotting in PARPi-resistant variants and parental Capan-1 cells. A stable vincristine (VCR)- resistant variant (KB/VCR) was a positive control of P-gp. (G and H) Cell lysates were

analyzed by Western blotting to determine PAR formation (G) and chromatin-bound PARP1 (H) triggered by MMS. Histone 3 was used as the positive control for the chromatin-bound fractions. TP, talazoparib. MMS, methyl methanesulfonate. (I and J) Simmiparib reduced H_2O_2-triggered PAR formation in both Capan-1/SP and Capan-1 cells. (I) Representative images of PAR formation. Nuclei were stained with DAPI. Scale bar, 100 μm. (J) Inhibitory curves and IC_{50} values of PAR formation inhibited by simmiparib in Capan-1/SP and Capan-1 cells. Data are presented as the mean ± SD from three independent experiments.

PARPi-resistant variants were consistently and irreversibly resistant to PARPi once established (Figure S1B).

Acquired resistance is not associated with P-gp, PARP activity, or PARP1-DNA trapping

Overexpression of drug transporters such as P-gp contributes to PARPi resistance [33]. However, the protein levels of BCRP and P-gp did not change in the PARPi-resistant variants relative to Capan-1 cells (**Figure 1E**). There was also no difference in the expression of PARP family members, particularly PARP1, PARP2, and PARP3, between the resistant and parental cells (**Figure 1F**). Moreover, there were no significant differences in PAR formation, PARP1-DNA trapping complexes driven by MMS, or the suppression of PAR formation by PARPi (**Figures 1G-J**, S1C, S1D). These data suggest that P-gp, PAR formation/inhibition, or PARP1-DNA trapping did not contribute to the acquired resistance in these PARPi-resistant variants.

Next-generation sequencing (NGS) identifies novel mutations in intron 11 of BRCA2 in PARPi-resistant sublines

Secondary intragenic mutations in mutated *BRCA2* are potential mechanisms underlying PARPi or cisplatin resistance in BRCA2-mutated cancers [11, 12]. First, we examined whether secondary mutations in the *BRCA2* gene, which result in the expression of a novel BRCA2 isoform, also occurred in our system. Capan-1 cells harbor a c.6174delT frameshift mutation at one of the alleles, which results in the expression of a truncated BRCA2 protein (recognized by Ab-1 of BRCA2; see **Figure 2A**). We used an antibody recognizing the C-terminal region of BRCA2 protein to detected possible new bands. As expected, a new BRCA2 isoform with a C-terminus (C-BRCA2 isoform) was identified in all three PARPi-resistant cells but not in parental cells (**Figure 2A**).

Next, mutational analysis of the *BRCA2* gene by genomic DNA sequencing and whole-exome sequencing were performed in all resistant and parental cells. Previous studies have revealed that secondary mutations resulting in a >2000 base pair (bp) intragenic deletion surrounding the c.6174delT mutation or exon 11/intron 11 junction restore the BRCA2 ORF [11, 12]. However, we did not identify any mutations surrounding the original c.6174delT mutation in the three resistant variants by NGS technology. Instead, we identified novel mutations in intron 11 of *BRCA2* with c.6841+2T>C or c.6841+1G>A in PARPi-resistant variants (Table S1). Concordance of the NGS results, mutations in intron 11 were also obtained with Sanger sequencing (**Figure 2B**). We also sequenced other genes commonly related to PARPi sensitivity including *PTEN*, *BRCA1*, *ATM*, and *TP53* and did not find *de novo* mutations in these genes (Table S1). In order to further determine the sequence of new isoforms found in **Figure 2A**, a seminested PCR using a panel of primers designed to amplify exon 11-containing isoforms was performed on exon 11-27 complementary DNA (cDNA) amplicons from parental and PARPi-resistant cells. The seminested PCR produced several electrophoretic bands in most of lanes, and sequencing of the cDNA from these bands revealed novel transcripts with in-frame deletions, corresponding in size to each of the BRCA2 isoforms (shown in **Figure 2B**, **2C**). The Capan-1/TP transcript 1 had an original c.6174delT frameshift mutation that encoded a truncated protein of BRCA2, similar to the parental cells; transcript 2 had a 4042-bp deletion and 83-bp insert; transcript 3 had a 4012-bp deletion and encoded a protein lacking amino acids 1722-3059; and transcript 4 had a 679-bp deletion (**Figure 2B**, **2C**). Capan-1/OP and Capan-1/SP also expressed *BRCA2* alleles harboring deletions of up to 4012 bp or 4009 bp. In all three resistant variants, the most prevalent transcripts with a 4012/4009-bp deletion corresponded in size to the C-terminal BRCA2 truncated protein, and these transcripts were not present in the parental Capan-1 or wild type BxPC3 cells. Therefore, transcripts with a 4012/4009-bp deletion were

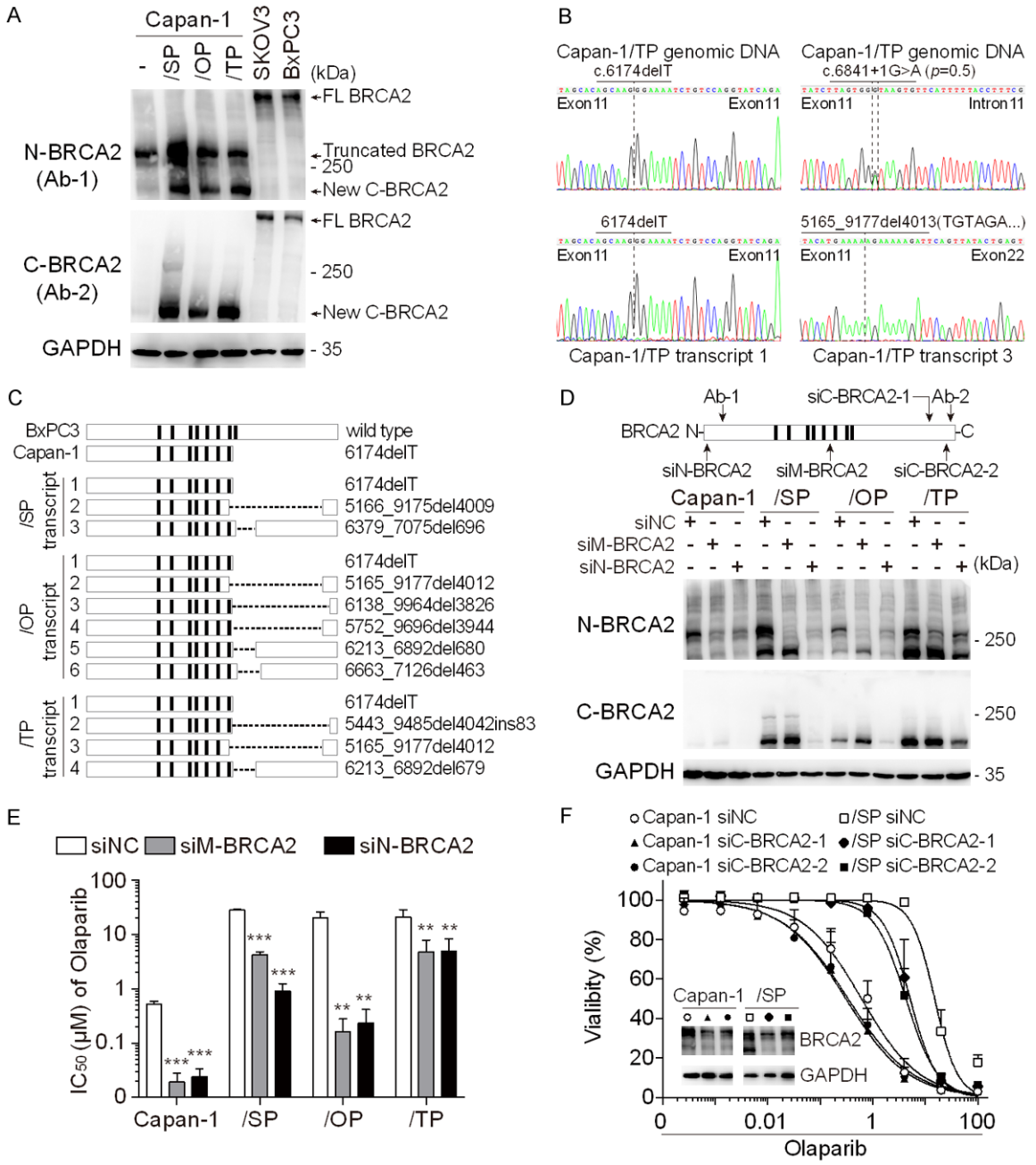

Figure 2. PARPi-resistant variants harbor secondary mutations in intron 11 of *BRCA2*. (A) Cell lysates from indicated cells were immunoblotted with anti-BRCA2 antibodies recognizing N-terminal BRCA2 (residues 450-500 (Ab-1)) or C-terminal BRCA2 (residues 3319-3418 (Ab-2)) epitopes. FL, full length. BxPC3 and SKOV-3 cells are shown as a positive control of full length BRCA2. (B) Representative validation of NGS data by Sanger sequencing and two BRCA2 transcripts in Capan-1/TP cells. In genomic DNA (upper), a homozygous exon mutation (c.6174delT) and a heterozygous intron mutation (c.6841+1G>A) were identified. In complimentary DNA (cDNA, lower), a homozygous mutation (6174delT) in exon11 and a homozygous 4013-bp deletion from exon 11 to exon 22 were identified. P = 0.5 means that mutant allele frequencies are 0.5. (C) Schematic presentation of BRCA2 full-length protein and new isoforms. BRCA2 isoforms were predicted from the cDNA and genomic sequences. Open boxes represent the cDNA of BRCA2. The filled boxes represent the BRC Repeats (1-8) region in the cDNA of BRCA2. And dotted lines represent missing regions predicted based on sequencing results. (D) Knockdown of BRCA2. Cells were transfected with siRNA, and BRCA2 expression was evaluated by Western blotting. Upper panel: regions that the BRCA2 antibodies (Ab-1 and Ab-2) recognize and the siRNA (siN-BRCA2 and siM-BRCA2) targets are depicted. (E, F) Olaparib sensitivity assessed by the SRB assay after cells were treated with the indicated siRNAs. Cells were transfected with siRNA specific to C-terminus of BRCA2, and knockdown of BRCA2 isoform by siC-BRCA2 was confirmed by western blotting (F). Depletion of BRCA2 with siM-BRCA2, siN-BRCA2 (E) and siC-BRCA2 (F) sensitized cells to Olaparib. Data are presented as the mean ± SD from three independent experiments. **P<0.01; ***P<0.001.

predicted to produce the new C-BRCA2 isoforms lacking 1337 or 1338 amino acids (**Figure 2C**). Although at least three distinct splice forms of BRCA2 have been found, only a prominent truncated protein was detected by Western Blot (**Figure 2A**), suggesting that most of the secondary mutations result in a splicing defect. Therefore, it is possible that novel BRCA2 isoforms arose from secondary mutations in intron 11 of the *BRCA2* gene, which resulted in a variable cleavage of BRCA2 pre-RNA during transcription.

To determine the function of the novel BRCA2 isoforms or c.6174delT truncated BRCA2 protein detected in the PARPi-resistant lines, we knocked down BRCA2 expression with siRNA targeting the N-terminus (siN-BRCA2), coding sequence (CDS)10 region in the middle (siM-BRCA2), and C-terminus (siC-BRCA2) of BRCA2 (**Figure 2D**, upper panel). The new isoform of BRCA2 was only downregulated by siN-BRCA2 but not by siM-BRCA2 (**Figure 2D**, lower band). Surprisingly, the c.6174delT truncated BRCA2 protein was knocked down by both siM-BRCA2 and siN-BRCA2, indicating that the CDS10 region may be important for the stability of this truncated protein (**Figure 2D**, upper band). Interestingly, blocking the c.6174delT truncated BRCA2 or new BRCA2 isoform using siN-BRCA2 and siM-BRCA2 significantly increased sensitivity to olaparib, simmiparib and talazoparib in both the parental and resistant cells (**Figures 2E** and S2A, S2B). Furthermore, the novel BRCA2 isoform was successfully knocked down with two pairs of siC-BRCA2 (**Figure 2F**). Consistently, interference with the C-BRCA2 isoform partially restored sensitivity of the PARPi-resistant variant but not the parental cells to the PARPi (**Figures 2F** and S2C). The resistance factors decreased from 24 to 16 and 12, respectively; in other words, silencing of the novel C-BRCA2 isoform caused decreased resistance to 32-49%. Next, we assessed the function of the new C-BRCA2 protein in the resistant cells by evaluating Rad51 foci formation after DNA damage. As previous reported, Ionizing radiation (IR) induced Rad51 foci formation was impaired in parental Capan-1 cells. In contrast, Capan-1/SP subline with restored C-BRCA2 expression, the IR-induced Rad51 foci formation was significant increased, suggesting that these novel C-BRCA2 isoform are functional. More importantly, knockdown of these C-BRCA2 isoforms apparently abrogated IR-induced Rad51 foci formation in Capan-1/SP cells (Figure S2D, S2E). Similarly, depletion of BRCA2 using the CRISPR/Cas9 technique, which truncated BRCA2 and led to almost complete disappearance of the new BRCA2 isoform, partially reversed resistance to the PARPi (Figure S2F, S2G). However, these functional studies revealed that only a fraction (32-49%) of the PARPi sensitivity could be rescued by depletion of the novel BRCA2 isoform. Collectively, these data suggest that the new BRCA2 isoform is one of key factors that mediate the resistance of cancer cells to PARPi, but the mechanisms underlying PARPi resistance are not fully understood.

PARPi-resistant variants accumulate a large amount of DSBs

DSBs are one of the most toxic lesions in human cells, and lead to genomic instability and cell death if left unrepaired [34]. Unexpectedly, we observed significantly higher levels of γH2AX and p-ATM in all three resistant cells compared to Capan-1 cells (**Figure 3A** and **3B**). The comet assay and the TUNEL assay showed that the DSBs were significantly higher in the resistance cells than in the parental cells (**Figure 3C-F**), indicating that the resistant cells harbors more spontaneous or unrepaired DSBs. The accumulation of unrepaired DNA damage can result in cell death or cellular senescence. Surprisingly, there were no apparent differences in cell survival rates between the parental and PARPi-resistant Capan-1 cells, as determined by Trypan Blue staining (**Figure 3G**, **3H**) and CellTiter-Glo cell viability assays (**Figure 3I**). In conclusion, although a higher amount of DSBs accumulated in the PARPi-resistant variants, there were no apparent effects on cell growth and survival.

However, when treated with an equivalent dosage of PARPi, all of the resistant variants failed to induce DNA damage, with apparent reduction of γH2AX accumulation and phosphorylated checkpoint kinase 1 (p-CHK1, Ser345) (Figure S3A and S3B). Similarly, treatments with simmiparib resulted in G2/M arrest, increased percentage of apoptotic population and activated caspase 3/9 in parental cells, but had no significant effects on Capan-1/SP cells (Figure S3C-E). In addition, no significant

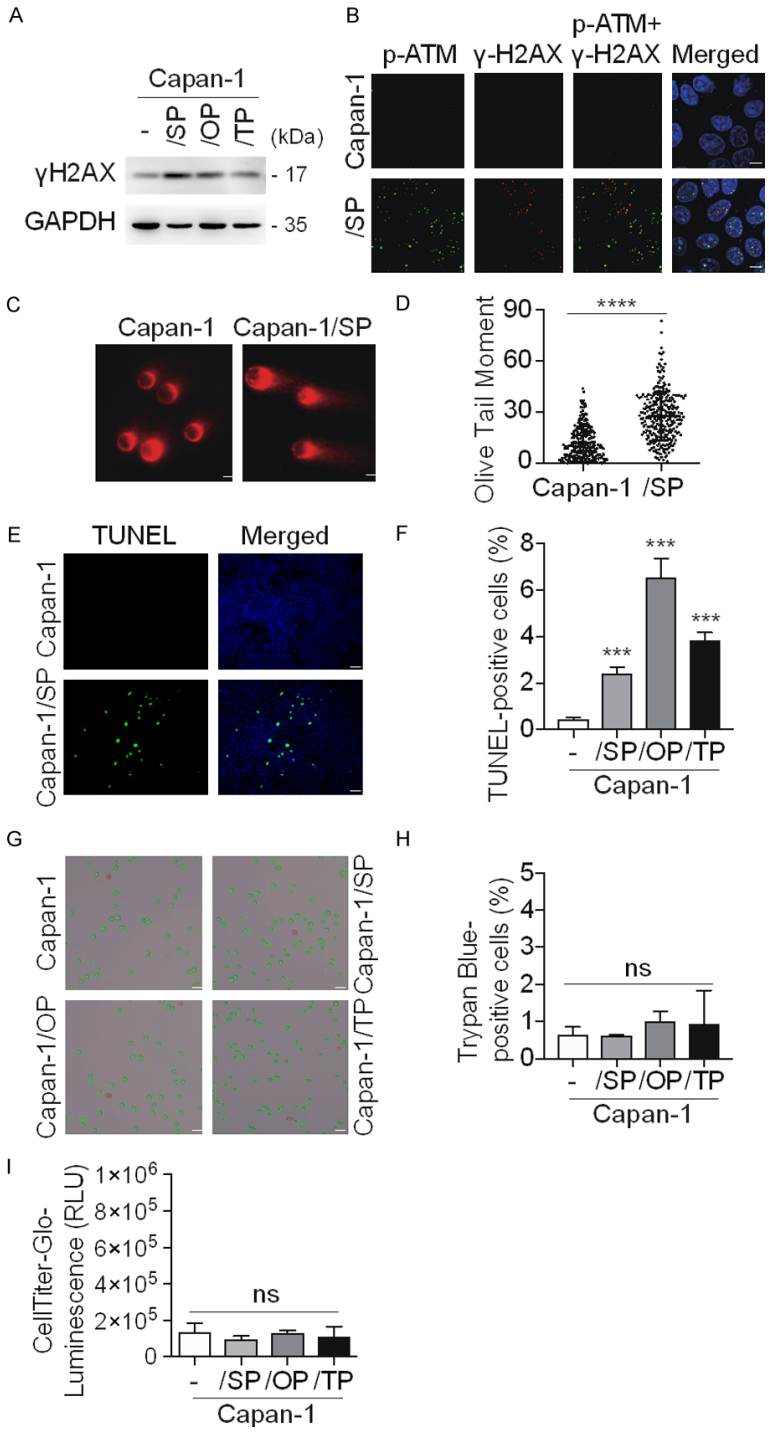

Figure 3. PARPi-resistant variants accumulate more intrinsic DNA damage than parental cells. (A) Levels of γH2AX protein were determined by Western blotting from PARPi-resistant variants and Capan-1 cells. (B) p-ATM and γH2AX staining of Capan-1/SP and Capan-1 cells. Scale bar, 5 μm. (C and D) DNA DSBs were detected by the two-tailed comet assay. Representative images (C), and quantitative data (D). Scale bar, 5 μm. Data are expressed as the mean ± SD from three independent experiments, n>250. (E and F, TUNEL staining of PARPi-resistant variants and Capan-1 cells. Representative images (E), and quantitative data (F). (G and H) Trypan blue staining of PARPi-resistant variants and Capan-1 cells. Trypan blue-positive cells are identified by a red circle mark. Representative images (G), and quantitative data (H). Scale bar, 30 μm. (I) Measuring cell viability using the CellTiter-Glo assay. Data are presented as the mean ± SD from three independent experiments. ***P<0.001; ****P<0.0001.

change in the levels of proteins associated with DNA damage repair was observed (Figure S3F).

PARPi-induced apoptosis is almost completely abrogated in the PARP-resistant cells

As mentioned above (Figure S3), low concentrations of PARPi, such as 1 μM olaparib or simmiparib, failed to induce DNA damage, cell cycle arrest and apoptosis in the resistant variants. To further investigate the relationship between DSB accumulation and cell death in PARP-resistant cells, equivalent effective concentrations were calculated and used for their treatment. As the IC_{50} reflects the cytotoxicity of PARPi, we used corresponding concentrations of 1 × IC_{50} or 2 × IC_{50} of olaparib to treat Capan-1/SP and parental cells (1 × IC_{50} and 2 × IC_{50}: 1.21 μM and 2.24 μM in Capan-1; 10.92 μM and 21.84 μM in Capan-1/SP). As expected, the use of equivalent olaparib concentrations caused an equal or even slight increase of γH2AX accumulation or p-Chk1 (Ser345) in Capan-1/SP-resistant sublines compared to the parental cells (**Figure 4A**). To exclude the interference of spontaneous DSBs, we quantified the amount of γH2AX- and p-ATM-positive cells, and found that the concentrations equivalent to respective IC_{50s} of olaparib re-

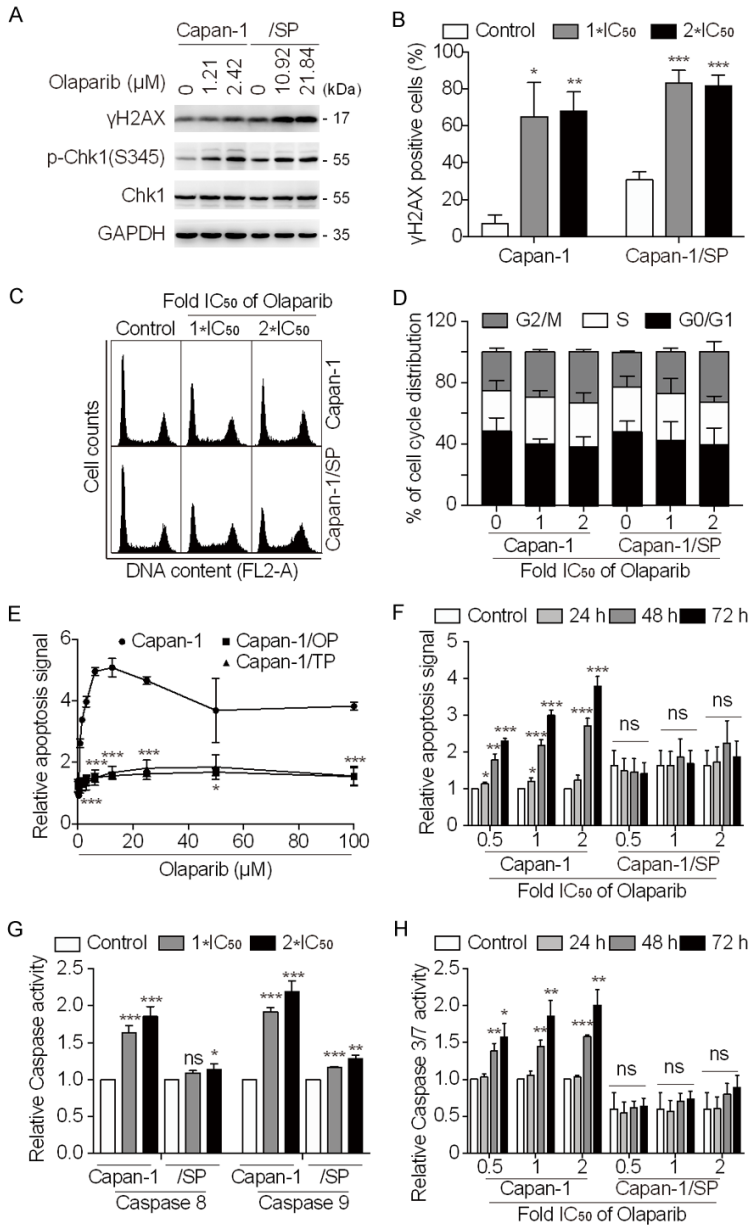

Figure 4. Equivalent concentration of olaparib failed to induce apoptosis in PARPi-resistant variants. (A) After exposure to 1 × IC_{50} or 2 × IC_{50} of olaparib, the indicated cells were subjected to immunoblotting analysis for γH2AX and p-Chk1. 1 × IC_{50} and 2 × IC_{50}: 1.21 μM and 2.24 μM in Capan-1; 10.92 μM and 21.84 μM in Capan-1/SP. (B) Quantitative analysis of γH2AX foci. Both Capan-1/SP and Capan-1 cells were treated with 1 × IC_{50} or 2 × IC_{50} olaparib for 48 h, and then subjected to immunofluorescence staining. Cells that contained five or more γH2AX foci per nucleus were considered γH2AX-positive cells. (C and D) G2/M phase arrest induced by equivalent olaparib was determined by flow cytometry. (C) Representative histograms; (D) Quantitative data from three independent experiments. (E-H) Equivalent concentration of olaparib was not able to induce apoptosis in PARPi-resistant cells. Capan-1, Capan-1/OP, and Capan-1/TP cells were exposed to increasing concentrations of olaparib for 72 h (E), or 24-72 h (F), and then the relative apoptosis signal was determined by the RealTime-Glo™ Annexin V Apoptosis Assay. Caspase 8/9 activity or caspase 3/7 activity was determined by the Caspase-Glo® 8, Caspase-Glo® 9 (G), or Caspase-Glo® 3/7 assay (H). Data are presented as the mean ± SD from three independent experiments. *P<0.05; **P<0.01; ***P<0.001.

sulted in almost the same percentage of γH2AX- and p-ATM-positive cells in both Capan-1/SP and Capan-1 cells (**Figures 4B** and S4A, S4B). Similarly, G2/M phase arrest induced by each IC_{50}-equivalent concentration of olaparib was almost the same in Capan-1/SP and Capan-1 cells (**Figure 4C**, **4D**). PARPi are known to kill tumor cells through induction of apoptosis [7, 23]. Next, we used the Realtime-Glo™ Annexin V Apoptosis Assay to monitor the progression of apoptosis induced by olaparib in Capan-1/OP, Capan-1/TP and Capan-1 cells. Surprisingly, the relative apoptosis signal quickly reached its peak at a very low concentration in Capan-1 (<20 μM), whereas there was almost no change in Capan-1/OP and Capan-1/TP cells at the concentrations as high as 100 μM (**Figure 4E**). Consistently, a 2-4 fold increase of apoptotic signals in concentration- and time-dependent manners was detected in the parental cells, but a much lower signal in Capan-1/SP cells was detected with treatments with the corresponding concentration of olaparib (**Figure 4F**). Furthermore, activation of caspases 8 and 9 was significantly higher in the parental cells than in Capan-1/SP cells treated with IC_{50}-equivalent concentrations of olaparib (**Figure 4G**). Similar results were revealed with regard to caspase 3 and 7 activation and loss of the mitochondrial membrane potential (MMP) (**Figures 4H** and S4C and S4D). Taken together, these data suggest that the apoptosis signals, including activation of caspases 3, 7, 8, 9 and depolarization of the MMP, are almost abrogated in the PARP-

resistant cells, although a large amount of DSBs remained upon spontaneous endogenous DNA damage or PARPi treatments.

Overexpression of COX-2/BIRC3 confers resistance to apoptosis in the PARPi-resistant variants

To investigate the molecular basis underlying apoptotic resistance in the PARPi-resistant variants, the expression patterns of the whole transcriptome were profiled using RNA sequencing (RNA-seq) to compare Capan-1/SP and Capan-1/OP cells with parental Capan-1 cells. Based on Gene Ontology functional analysis, several components of the anti-apoptotic complexes such as COX-2 and BIRC3 showed increased transcription levels in the PARPi-resistant variants (Table S2). COX-2 is involved in drug resistance and the poor prognosis of many neoplastic diseases and cancers [35]. BIRC3 (c-IAP2), a type of IAP protein, promotes cell survival and prevents activation of apoptosis by interfering with caspase activation [25]. We validated that all three resistant variants expressed much more COX-2 (9-52 fold) and BIRC3 (4-8 fold) mRNA (**Figure 5A**) and proteins (**Figure 5B**) than the parental cells. Importantly, knockdown of COX-2 or BIRC3 by RNAi (**Figure 5C**) significantly restored the sensitivity of Capan-1/SP to olaparib with the resistance factors decreasing from 19 to 5-14 or 6-12 and caused a reduction in drug resistance up to 72% or 70%, respectively (**Figure 5D** and **5E**). Similar results were observed using simmiparib (Figure S5A). Interestingly, siRNA co-targeting COX-2 and BIRC3 did not produce additive effects on the re-sensitivity of Capan-1/SP to PARPi (**Figures 5E** and S5A), indicating that there was certain overlapping in the functions between these two proteins. Unexpectedly, simultaneous depletion of the BRCA2 mutant and suppression of COX2/BIRC3 did not caused additive effects of restoration (Figure S5B). We previously generated a PARPi-resistant glioblastoma U251/OP cells by olaparib exposure [29]. Indeed, COX-2 levels were found to be significantly increased in U251/OP cells when compared to parental cells (shown in **Figure 6F**). A similar effect of COX-2 inhibition that restored the sensitivity to PARPi was also observed in U251/OP cells (Figure S5C and S5D). Depletion of COX-2 and BIRC3 significantly increased the apoptosis signaling triggered by olaparib (**Figure 5F**). Thus, targeting COX-2 and BIRC3 may overcome apoptotic resistance in PARPi-resistant variants. PGE2 is a major metabolic product of COX-2 [36]. Exogenous addition of 10 μM PGE2 significantly reduced the apoptotic signals increased by olaparib in Capan-1 cells (**Figure 5G**). As expected, the ectopic expression of COX2 significantly reduced the sensitivity of Capan-1 or U251 cells to PARPi (**Figures 5H**, S5E and S5F). Combination of the BIRC3 inhibitor LCL161 with the PARPi led to a clear decrease in viability of the Capan-1/SP cells, and up to 2.98-fold re-sensitivity compared with olaparib or simmiparib alone (Figure S5G and S5H). These data suggest that COX-2 and BIRC3 appear to jointly regulate the apoptosis pathway and promote the cell survival of resistant sublines, whereas silencing COX-2 or BIRC3 results in the re-sensitization of PARPi-resistant cells to the PARPi. Therefore, we conclude that the overexpression of COX-2 and BIRC3 may contribute to the decreased PARPi response and confer apoptotic resistance in PARPi-resistant variants.

PARP1 negatively regulates COX-2 and BIRC3 expression

Accumulating evidence has suggested that PARP1 plays an important role in the regulation of gene expression, although the mechanisms still remain unclear [37]. To determine whether the overexpression of COX-2 and BIRC3 in PARPi-resistant variants may also be linked to transcriptional regulation *via* ADP-ribosylation of PARP1, we measured the mRNA levels of these genes in Capan-1 cells upon depletion or chemical inhibition of PARP1. As expected, olaparib, simmiparib and talazoparib caused a concentration-dependent increase in the mRNA expression of COX-2 and BIRC3 (**Figure 6A**), and upregulation of the protein levels (**Figure 6B**). The expression of COX-2 and BIRC3 was upregulated with a peak at 72 h PARPi treatments but decreased after washing off PARPi for 3 or 6 days (Figure S6A). The increased mRNA or protein expression of COX-2 and BIRC3 was also observed in RD-ES Ewing's sarcoma cells (Figure S6B and S6C) and U251 cells (Figure S6D). Furthermore, after genetic depletion of PARP1, we observed a significant increase in the mRNA (**Figure 6C**) and protein levels (**Figure 6D**) of COX-2 and BIRC3 in PARP1$^{-/-}$ cells of Capan-1 and RD-ES [31]. Similar results were obtained in PARPi-resistant variants of RD-ES and U251 cells (**Figures 6E**, **6F**

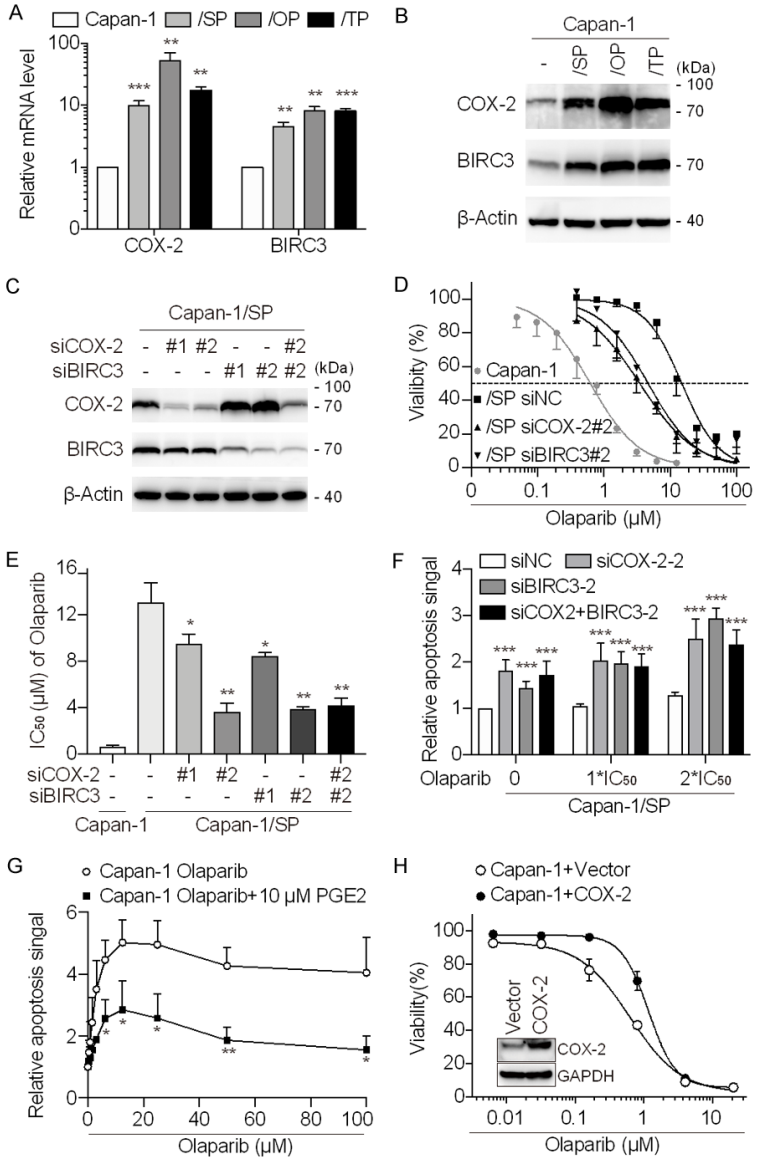

Figure 5. Depletion of COX-2 or BIRC3 partially restores the sensitivity of PARPi-resistant variants to PARPi. A. The mRNA level of COX-2 or BIRC3 was detected by qPCR in three PARPi-resistant variants and Capan-1 cells. Data are normalized and presented as the mean ± SD. B. The upregulation of COX-2 and BIRC3 in PARPi-resistant variants was confirmed by western blotting. C. Capan-1/SP cells were transfected with siCOX-2 or siBIRC3 or both for 72 h, and then subjected to western blotting. D and E. Knockdown of COX-2 or BIRC3 re-sensitized Capan1-/SP cells to olaparib. After transfection with the indicated siRNA, cells were treated with olaparib for 7 days and then subjected to SRB assays. D. Survival curves of olaparib-treated cells. E. IC_{50} values of olaparib presented as the mean ± SD from three independent experiments. F. Knockdown of COX-2 or BIRC3 partially rescued the apoptosis signaling of Capan1-/SP cells to olaparib. After transfection with the indicated siRNA, cells were treated with olaparib for 72 h and then the relative apoptosis signal was detected using the RealTime-Glo™ Annexin V Apoptosis Assay. G. Capan-1 cells were treated with olaparib alone or combined with 10 μM PGE2 for 72 h, followed by subsequent detection of the relative apoptosis signal by RealTime-Glo™ Annexin V Apoptosis Assay. H. Exogenous expression of COX-2 in Capan-1 cells reduced olaparib sensitivity. Cells were infected by MOI = 5, the levels of COX-2 protein were determined by Western blotting, then cell viability was assessed by SRB assays with olaparib for 7 days. Data are presented as the mean ± SD from three independent experiments. *P<0.05; **P<0.01; ***P<0.001.

and S6E), suggesting that their expression was negatively regulated by PARP1 in various tumor cells. These data indicate that PARP1 is a novel negative transcriptional regulator of COX-2 and BIRC3. We proposed that depletion or chemical inhibition of PARP1 triggers the upregulation of COX-2/BIRC3 mRNA and protein, and subsequent development of resistance to PARPi-induced apoptosis.

Discussion

Studies on PARPi agents have initially focused on BRCA1/2-mutated tumors defective for HRR in the clinic, and restoration of HRR appears to be the predominant mechanism of resistance to PARPi [1]. In this study, we generated three different PARPi-resistant cells (Capan-1/OP, Capan-1/SP, and Capan-1/TP) by chronically treating Capan-1 cells with increasing concentrations of olaparib, simmiparib or talazoparib. Our data demonstrated that even derived from different PARPi, secondary mutations were found in the intron 11 of *BRCA2* and resulted in expression of a novel BRCA2 isoform in all three resistant cells. However, depletion of this novel C-BRCA2 isoform only restored partial resistance to the PARPi. Our study further revealed that apoptotic resistance driven by COX-2 and BIRC3 overexpression also played an important role in

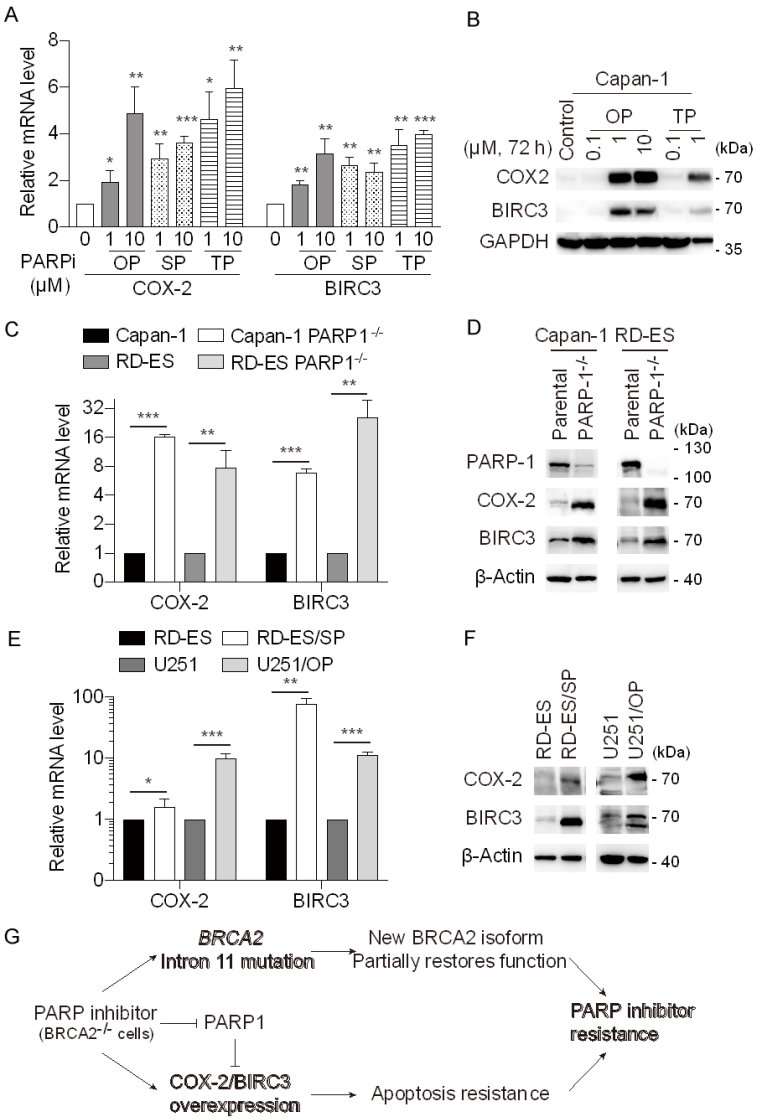

Figure 6. PARPi or PARP1 depletion induces upregulation of COX-2/BIRC3 expression. (A) Capan-1 cells were treated with olaparib (OP), simmiparib (SP) and talazoparib (TP) for 48 h, and then relative mRNA levels of COX-2 and BIRC3 were determined by qPCR. (B) Protein levels of COX-2 and BIRC3 were detected by western blotting after 72 h olaparib (OP) and talazoparib (TP) treatment in Capan-1 cells. (C and D) PARP1 was stably knocked down by CRISPR/Cas9 or TALEN in Capan-1 or RD-ES cells [31], and the mRNA levels (C) and protein levels (D) of COX-2 and BIRC3 were determined by qPCR and Western blotting. (E and F) PARPi-resistant variants of RD-ES or U251 [29], and the mRNA levels (E) and protein levels (F) of COX-2 and BIRC3 were determined by qPCR and Western blotting. Data are presented as the mean ± SD from three independent experiments. *P<0.05; **P<0.01; ***P<0.001. (G) Schematic model to show formation of PARPi resistance in pancreatic cancer Capan-1 cells. When chronically treated with increasing concentration of PARPi, cancer cells develop two distinct pathways to overcome PARPi cytotoxicity. Under selective pressure of PARPi exposure, BRCA2-mutated cancer cells acquired new mutations in intron 11 of BRCA2, which restored expression of the functional novel BRCA2 protein. Meanwhile, PARPi treatment significantly increased anti-apoptotic gene (COX-2 and BIRC3) expression by inhibiting PARP-1, thereby suppressing apoptosis by COX-2/PGE2/BIRC3 and promoting cell survival under DSBs. As a result, cells with secondary mutations and apoptotic resistance were significantly resistant to PARPi.

PARPi resistance, as COX-2 or BIRC3 knockdown significantly increased the sensitivity of resistant variants to PARPi. In addition, PARP1 negatively regulated COX-2 and BIRC3 expression. Therefore, we hypothesized that the BRCA2 isoform caused by new mutations in intron 11 of *BRCA2*, and apoptotic resistance mediated by COX-2/BIRC3 overexpression each uniquely contributed to the chronic PARPi resistance (**Figure 6F**).

In BRCA1/2-mutated tumors, regaining BRCA function through back mutation, reading frame restoration, or loss of promoter methylation is considered the primary resistance mechanism [1, 38]. Loss of 53BP1-RIF1-REV7, bypassing the need of BRCA1 for HR activity, is another well-described mechanism of resistance to PARPi [19, 20, 39]. Among these, novel truncated BRCA2 isoforms caused by intragenic deletions in BRCA2 are frequently associated with resistance to PARPi in BRCA2-deficient cells. In Capan-1 or HCC1428 cells, secondary genetic changes include in-frame deletions (2135 bp) surrounding the original 6174delT mutation site and the exon 11/in intron 11 junction [12], large deletions of up to 58 kb [11], and a small deletion (~5 bp) [40] at sites close to the original mutation. We speculated that new mutations may occur in the original mutation site and intron 11 regions, and mutations in these two genetic susceptibility regions may lead to spliced or truncated BRCA2 isoforms. In our *in vitro* system, all three Capan-1 PARPi-resistant variants did not harbor deletions surrounding the 6174delT mu-

tation or at the exon 11/intron 11 junction as previously reported [11, 12]. Instead, they harbored new mutations in intron 11 of *BRCA2*; for example, Capan-1/SP and Capan-1/OP harbored the c.6841+2T>C mutation, but Capan-1/TP harbored the c.6841+1G>A mutation. The first two base sequences G and T at the 5' splice site of the intron are key intron splicing signals, and mutations at this region can affect pre-mRNA splicing and other RNA processing reactions [41, 42]. We proposed that new mutations at the first two sites of intron 11 result in the expression of novel splice transcripts with in-frame deletions, and subsequently produce new C-terminal BRCA2 isoforms. However, additional studies are needed to determine how intron 11 mutations cause the formation of new BRCA2 alternative spliceosomes and to elucidate the underlying regulatory mechanisms. In this study, because Capan-1 cells were similarly exposed to increasing concentrations of PARPi for several months to obtain resistant sublines with a resistance factor up to >1000 fold, we were interested in determining why the secondary genetic mutations identified in our system were different from previous studies. We speculated that first, the secondary mutations caused by different DNA-damaging drugs may vary e.g., *BRCA2* mutation or deletion caused by KU0058948 differ with cisplatin, talazoparib, olaparib and simmiparib treatment [11, 12]. Second, investigators have selected different exposure times to PARPi. We showed that depletion of novel isoforms partially restored sensitivity of the PARPi-resistant variants to PARPi by only approximately 32.22-49.03%, although depletion of novel isoforms of BRCA2 apparently abrogated its function. This strongly suggesting that additional proteins that function in PARPi resistance remain to be identified.

γH2AX is a well-characterized early marker of DNA damage and is frequently used as a marker reflecting PARPi cytotoxicity [7, 29, 43]. We previously reported that the PARPi inhibitors olaparib and simmiparib, induced DNA lesions, cell cycle arrest, and caspase-dependent apoptosis of BRCA-deficient cells *in vitro* [6, 7, 21-23]. Surprisingly, we found that the accumulation of DSBs was significantly higher in PARPi-resistant variants than in parental cells, but did not affect cell survival. These data indicated that PARPi-resistant variants showed tolerance to DSBs. ATM-deficient cells harboring large numbers of DSBs have demonstrated resistance to apoptosis, and apoptosis-resistant spermatogonial stem cells accumulate DNA damage [44-46]. Apoptotic resistance might also occur in PARPi-resistant variants. We further observed that in the presence of equivalent concentrations of olaparib, the induced apoptosis signals (PS eversion, caspase 3/7/8/9 activation, and MMP loss) were almost completely abrogated in the resistant variants, although γH2AX and G2/M phase arrest was comparable between Capan-1/SP and parental cells. Apoptosis resistance is thought to be responsible for resistance to chemotherapy [47], but its role in PARPi resistance remains unknown. The observations from our study raise the possibility that apoptotic resistance contributes to the drug resistance of PARPi.

PARP1 plays important roles in both DNA repair and transcriptional regulation, but little is known about how one process affects the other [1, 37]. Yan Lin *et al.* [48] reported that PARP1 negatively regulates the transcriptional expression of COX-2 via binding to the inhibitory element. Whether this transcriptional regulation by PARP1 facilitates cytotoxicity or resistance to PARPi remains to be clarified. COX-2 overexpression-mediated apoptotic resistance can lead to resistance to multiple anticancer therapy, such as imatinib [49], cisplatin [50], cetuximab [51], ursolic acid [52], ultraviolet B [53], and radiation [54], which is usually associated with increasing levels of Mcl-1 or inhibition of the p53 pathway [49, 53]. In addition, overexpression of other anti-apoptotic proteins, such as BIRC2, BIRC3 and Bcl-2, are associated with resistance to DNA-damaging agents [24, 55], suggesting the possibility of negative crosstalk between DNA lesions and apoptosis. In this study, we demonstrated that chronic PARP inhibition resulted in a marked increase in the mRNA and protein levels of COX-2 and BIRC3. Most importantly, interfering with COX-2 or BIRC3 significantly re-sensitized Capan-1/SP to olaparib by up to 72% or 70%, but did not produce additive effects when both were co-targeted. Surprisingly, when simultaneous depletion of BRCA2 mutant and suppression of COX2/BIRC3, there was no additive effect of restoration. We proposed that these two causes may be a partly overlapping in function and contribute to PARPi resistance. Similarly,

knockdown of these two genes significantly rescued the apoptotic signaling trigged by the PARPi. Further evidence showed that the mRNA levels of COX-2 and BIRC3 significantly increased in a concentration-dependent manner upon PARPi treatment or PARP1 depletion, suggesting the presence of a negative feedback loop which limits the cytotoxicity of long-term PARP inhibition. Our data revealed that PARP1 is a novel negative transcriptional regulator of COX-2 and BIRC3. A previous study demonstrated that PARP1 suppresses the transcriptional expression of COX-2 through binding to the repressor element in the promoter region of COX-2 [48]; however, the processes involved in the transcriptional regulation of BIRC3 remain unknown. We propose that COX-2 and BIRC3 cooperate to drive tumor growth, survival, and apoptotic resistance to PARP inhibition. Thus, drug combinations co-targeting COX-2 and BIRC3 may offer valid therapeutic approaches for overcoming resistance to PARPi. Consistent with this notion, the combination of PARPi and the BIRC3 inhibitor LCL161 has been shown to significantly improve the antitumor effect. Upregulation of COX-2 and BIRC3 expression upon PARPi treatments was observed in resistant sublines of BRCA2-mutant Capan-1 pancreatic cells, RD-ES Ewing's sarcoma cells and PTEN-deficient U251 glioblastoma cells (**Figure 6**). These data strongly suggest that overexpression of COX-2 and BIRC3 is a relatively universal mechanism responsible for PARPi resistance.

However, several important issues remain to be clarified, such as what are the heritable genetic changes, how the persistent PARPi exposure causes them and how they lead to upregulation of COX-2 and BIRC3 expression. PARP1-mediated transcriptional regulation is complicated and unpredictable. Previous studies revealed that PARP1 regulated gene transcription in several ways, including dependent on or independent of its polymerase activity and varies in different gene or cell type [56]. In this study, PARPi caused upregulation of COX-2 and BIRC3 in both cells after long-term (>100 days) or relative short-time (48 h) exposure to PARPi. Moreover, knockout of PARP1 markedly increased COX-2 and BIRC3. These data indicated that COX-2 and BIRC3 may be regulated by PARP1 directly in a manner of polymerase-activity dependence. Recently, a new PARP1-gene promoter binding mode has been clarified in our lab [57]; and applying the similar techniques, how PARP1 represses the transcriptional expression of COX2/BIRC3 would be further explored.

In conclusion, we demonstrate that novel *BRCA2* intron 11 mutations and COX-2/BIRC3-mediated apoptotic resistance jointly promote the survival of Capan-1 cancer cells upon chronic PARPi exposure. The results also reveal that different PARPi have similar drug resistance characteristics, leading to cross-resistance to other PARPi. These findings provide novel insights into how to overcome resistance to PARPi.

Acknowledgements

This work was supported by grants from the National Natural Science Foundation of China (81573450 to Z.H. Miao and 81603160 and 81773764 to J.X. He), the Chinese Academy of Sciences (29201731121100101 and XDA-12010306 to J.X. He and XDA12020104, XDA12020109 and CASIMM0120185003 to Z.H. Miao), the Science and Technology Commission of Shanghai Municipality (19QA-1410900 to J.X. He and 16JC1406300 to Z.H. Miao), the State Key Laboratory of Drug Research, the Open Studio for Drugability Research of Marine Natural Products in the Qingdao Pilot National Laboratory for Marine Science and Technology, and SA-SIBS Scholarship Program.

Disclosure of conflict of interest

None.

Address correspondence to: Drs. Jin-Xue He and Ze-Hong Miao, Division of Antitumor Pharmacology, State Key Laboratory of Drug Research, Shanghai Institute of Materia Medica, Chinese Academy of Sciences, Shanghai 201203, P. R. China. Tel: +86-21-50800709; Fax: +86-21-50800709; E-mail: jinxue_he@simm.ac.cn (JXH); zhmiao@simm.ac.cn (ZHM)

References

[1] Wang YQ, Wang PY, Wang YT, Yang GF, Zhang A and Miao ZH. An update on poly(ADP-ribose) polymerase-1 (PARP-1) inhibitors: opportunities and challenges in cancer therapy. J Med Chem 2016; 59: 9575-9598.

[2] He JX, Yang CH and Miao ZH. Poly(ADP-ribose) polymerase inhibitors as promising cancer therapeutics. Acta Pharmacol Sin 2010; 31: 1172-1180.
[3] Syed YY. Rucaparib: first global approval. Drugs 2017; 77: 585-592.
[4] Scott LJ. Niraparib: first global approval. Drugs 2017; 77: 1029-1034.
[5] Hoy SM. Talazoparib: first global approval. Drugs 2018; 78: 1939-1946.
[6] He JX, Wang M, Huan XJ, Chen CH, Song SS, Wang YQ, Liao XM, Tan C, He Q, Tong LJ, Wang YT, Li XH, Su Y, Shen YY, Sun YM, Yang XY, Chen Y, Gao ZW, Chen XY, Xiong B, Lu XL, Ding J, Yang CH and Miao ZH. Novel PARP1/2 inhibitor mefuparib hydrochloride elicits potent in vitro and in vivo anticancer activity, characteristic of high tissue distribution. Oncotarget 2017; 8: 4156-4168.
[7] Yuan B, Ye N, Song SS, Wang YT, Song Z, Chen HD, Chen CH, Huan XJ, Wang YQ, Su Y, Shen YY, Sun YM, Yang XY, Chen Y, Guo SY, Gan Y, Gao ZW, Chen XY, Ding J, He JX, Zhang A and Miao ZH. Poly(ADP-ribose)polymerase (PARP) inhibition and anticancer activity of simmiparib, a new inhibitor undergoing clinical trials. Cancer Lett 2017; 386: 47-56.
[8] Pishvaian MJ, Biankin AV, Bailey P, Chang DK, Laheru D, Wolfgang CL and Brody JR. BRCA2 secondary mutation-mediated resistance to platinum and PARP inhibitor-based therapy in pancreatic cancer. Br J Cancer 2017; 116: 1021-1026.
[9] Gornstein EL, Sandefur S, Chung JH, Gay LM, Holmes O, Erlich RL, Soman S, Martin LK, Rose AV, Stephens PJ, Ross JS, Miller VA, Ali SM and Blau S. BRCA2 reversion mutation associated with acquired resistance to olaparib in estrogen receptor-positive breast cancer detected by genomic profiling of tissue and liquid biopsy. Clin Breast Cancer 2018; 18: 184-188.
[10] Kondrashova O, Nguyen M, Shield-Artin K, Tinker AV, Teng NNH, Harrell MI, Kuiper MJ, Ho GY, Barker H, Jasin M, Prakash R, Kass EM, Sullivan MR, Brunette GJ, Bernstein KA, Coleman RL, Floquet A, Friedlander M, Kichenadasse G, O'Malley DM, Oza A, Sun J, Robillard L, Maloney L, Bowtell D, Giordano H, Wakefield MJ, Kaufmann SH, Simmons AD, Harding TC, Raponi M, McNeish IA, Swisher EM, Lin KK and Scott CL; AOCS Study Group. Secondary somatic mutations restoring RAD51C and RAD51D associated with acquired resistance to the PARP inhibitor rucaparib in high-grade ovarian carcinoma. Cancer Discov 2017; 7: 984-998.
[11] Edwards SL, Brough R, Lord CJ, Natrajan R, Vatcheva R, Levine DA, Boyd J, Reis-Filho JS and Ashworth A. Resistance to therapy caused by intragenic deletion in BRCA2. Nature 2008; 451: 1111-1115.
[12] Sakai W, Swisher EM, Karlan BY, Agarwal MK, Higgins J, Friedman C, Villegas E, Jacquemont C, Farrugia DJ, Couch FJ, Urban N and Taniguchi T. Secondary mutations as a mechanism of cisplatin resistance in BRCA2-mutated cancers. Nature 2008; 451: 1116-1120.
[13] Meghani K, Fuchs W, Detappe A, Drane P, Gogola E, Rottenberg S, Jonkers J, Matulonis U, Swisher EM, Konstantinopoulos PA and Chowdhury D. Multifaceted impact of microRNA 493-5p on genome-stabilizing pathways induces platinum and PARP inhibitor resistance in BRCA2-mutated carcinomas. Cell Rep 2018; 23: 100-111.
[14] Rondinelli B, Gogola E, Yücel H, Duarte AA, van de Ven M, van der Sluijs R, Konstantinopoulos PA, Jonkers J, Ceccaldi R, Rottenberg S and D'Andrea AD. EZH2 promotes degradation of stalled replication forks by recruiting MUS81 through histone H3 trimethylation. Nat Cell Biol 2017; 19: 1371-1378.
[15] Lai X, Broderick R, Bergoglio V, Zimmer J, Badie S, Niedzwiedz W, Hoffmann JS and Tarsounas M. MUS81 nuclease activity is essential for replication stress tolerance and chromosome segregation in BRCA2-deficient cells. Nat Commun 2017; 8: 15983.
[16] Ray Chaudhuri A, Callen E, Ding X, Gogola E, Duarte AA, Lee JE, Wong N, Lafarga V, Calvo JA, Panzarino NJ, John S, Day A, Crespo AV, Shen B, Starnes LM, de Ruiter JR, Daniel JA, Konstantinopoulos PA, Cortez D, Cantor SB, Fernandez-Capetillo O, Ge K, Jonkers J, Rottenberg S, Sharan SK and Nussenzweig A. Replication fork stability confers chemoresistance in BRCA-deficient cells. Nature 2016; 535: 382-387.
[17] Patch AM, Christie EL, Etemadmoghadam D, Garsed DW, George J, Fereday S, Nones K, Cowin P, Alsop K, Bailey PJ, Kassahn KS, Newell F, Quinn MC, Kazakoff S, Quek K, Wilhelm-Benartzi C, Curry E and Leong HS; Australian Ovarian Cancer Study Group, Hamilton A, Mileshkin L, Au-Yeung G, Kennedy C, Hung J, Chiew YE, Harnett P, Friedlander M, Quinn M, Pyman J, Cordner S, O'Brien P, Leditschke J, Young G, Strachan K, Waring P, Azar W, Mitchell C, Traficante N, Hendley J, Thorne H, Shackleton M, Miller DK, Arnau GM, Tothill RW, Holloway TP, Semple T, Harliwong I, Nourse C, Nourbakhsh E, Manning S, Idrisoglu S, Bruxner TJ, Christ AN, Poudel B, Holmes O, Anderson M, Leonard C, Lonie A, Hall N, Wood S, Taylor DF, Xu Q, Fink JL, Waddell N, Drapkin R, Stronach E, Gabra H, Brown R, Jewell A, Nagaraj SH, Markham E, Wilson PJ, Ellul J, McNally O, Doyle MA, Vedururu R, Stewart C, Lengyel E, Pearson JV, Waddell N, deFazio A, Grimmond SM and

Bowtell DD. Whole-genome characterization of chemoresistant ovarian cancer. Nature 2015; 521: 489-494.

[18] Guillemette S, Serra RW, Peng M, Hayes JA, Konstantinopoulos PA, Green MR and Cantor SB. Resistance to therapy in BRCA2 mutant cells due to loss of the nucleosome remodeling factor CHD4. Genes Dev 2015; 29: 489-494.

[19] Jaspers JE, Kersbergen A, Boon U, Sol W, van Deemter L, Zander SA, Drost R, Wientjens E, Ji J, Aly A, Doroshow JH, Cranston A, Martin NM, Lau A, O'Connor MJ, Ganesan S, Borst P, Jonkers J and Rottenberg S. Loss of 53BP1 causes PARP inhibitor resistance in Brca1-mutated mouse mammary tumors. Cancer Discov 2013; 3: 68-81.

[20] Xu G, Chapman JR, Brandsma I, Yuan J, Mistrik M, Bouwman P, Bartkova J, Gogola E, Warmerdam D, Barazas M, Jaspers JE, Watanabe K, Pieterse M, Kersbergen A, Sol W, Celie PH, Schouten PC, van den Broek B, Salman A, Nieuwland M, de Rink I, de Ronde J, Jalink K, Boulton SJ, Chen J, van Gent DC, Bartek J, Jonkers J, Borst P and Rottenberg S. REV7 counteracts DNA double-strand break resection and affects PARP inhibition. Nature 2015; 521: 541-544.

[21] Chen WH, Guo N, Qi MH, Dai HY, Hong MH, Guan LF, Huan XJ, Song SS, He JX, Wang YQ, Xi Y, Yang XY, Shen YY, Su Y, Sun YM, Gao YL, Chen Y, Ding J, Tang Y, Ren GB, Miao ZH and Li J. Discovery, mechanism and metabolism studies of 2,3-difluorophenyl-linker-containing PARP1 inhibitors with enhanced in vivo efficacy for cancer therapy. Eur J Med Chem 2017; 138: 514-531.

[22] Gaymes TJ, Shall S, MacPherson LJ, Twine NA, Lea NC, Farzaneh F and Mufti GJ. Inhibitors of poly ADP-ribose polymerase (PARP) induce apoptosis of myeloid leukemic cells: potential for therapy of myeloid leukemia and myelodysplastic syndromes. Haematologica 2009; 94: 638-646.

[23] Franzese E, Centonze S, Diana A, Carlino F, Guerrera LP, Di Napoli M, De Vita F, Pignata S, Ciardiello F and Orditura M. PARP inhibitors in ovarian cancer. Cancer Treat Rev 2018; 73: 1-9.

[24] Hassan M, Watari H, AbuAlmaaty A, Ohba Y and Sakuragi N. Apoptosis and molecular targeting therapy in cancer. BioMed Res Int 2014; 2014: 150845.

[25] Fulda S and Vucic D. Targeting IAP proteins for therapeutic intervention in cancer. Nat Rev Drug Discov 2012; 11: 109-124.

[26] Zhang L and Fang B. Mechanisms of resistance to TRAIL-induced apoptosis in cancer. Cancer Gene Ther 2005; 12: 228-237.

[27] Pang LY, Hurst EA and Argyle DJ. Cyclooxygenase-2: a role in cancer stem cell survival and repopulation of cancer cells during therapy. Stem Cells Int 2016; 2016: 2048731.

[28] Ye N, Chen CH, Chen T, Song Z, He JX, Huan XJ, Song SS, Liu Q, Chen Y, Ding J, Xu Y, Miao ZH and Zhang A. Design, synthesis, and biological evaluation of a series of benzo[de][1,7]naphthyridin-7(8H)-ones bearing a functionalized longer chain appendage as novel PARP1 inhibitors. J Med Chem 2013; 56: 2885-2903.

[29] Wang YT, Yuan B, Chen HD, Xu L, Tian YN, Zhang A, He JX and Miao ZH. Acquired resistance of phosphatase and tensin homolog-deficient cells to poly(ADP-ribose) polymerase inhibitor and Ara-C mediated by 53BP1 loss and SAMHD1 overexpression. Cancer Sci 2017; 109: 821-831.

[30] Chen WH, Song SS, Qi MH, Huan XJ, Wang YQ, Jiang HL, Ding J, Ren GB, Miao ZH and Li J. Discovery of potent 2,4-difluoro-linker poly(ADP-ribose) polymerase 1 inhibitors with enhanced water solubility and in vivo anticancer efficacy. Acta Pharmacol Sin 2017; 38: 1521-1532.

[31] Chen HD, Chen CH, Wang YT, Guo N, Tian YN, Huan XJ, Song SS, He JX and Miao ZH. Increased PARP1-DNA binding due to autoPARylation inhibition of PARP1 on DNA rather than PARP1-DNA trapping is correlated with PARP1 inhibitor's cytotoxicity. Int J Cancer 2019; 145: 714–727.

[32] Cortes-Gutierrez EI, Fernandez JL, Davila-Rodriguez MI, Lopez-Fernandez C and Gosálvez J. Two-tailed comet assay (2T-comet): simultaneous detection of DNA single and double strand breaks. Methods Mol Biol 2017; 1560: 285-293.

[33] Durmus S, Sparidans RW, van Esch A, Wagenaar E, Beijnen JH and Schinkel AH. Breast cancer resistance protein (BCRP/ABCG2) and P-glycoprotein (P-GP/ABCB1) restrict oral availability and brain accumulation of the PARP inhibitor rucaparib (AG-014699). Pharm Res 2014; 32: 37-46.

[34] Mladenov E, Magin S, Soni A and Iliakis G. DNA double-strand-break repair in higher eukaryotes and its role in genomic instability and cancer: cell cycle and proliferation-dependent regulation. Semin Cancer Biol 2016; 37-38: 51-64.

[35] Li W, Cao Y, Xu J, Wang Y, Li W, Wang Q, Hu Z, Hao Y, Hu L, Sun Y, Xu G and Ao G. YAP transcriptionally regulates COX-2 expression and GCCSysm-4 (G-4), a dual YAP/COX-2 inhibitor, overcomes drug resistance in colorectal cancer. J Exp Clin Cancer Res 2017; 36: 144.

[36] Semaan J, Pinon A, Rioux B, Hassan L, Limami Y, Pouget C, Fagnere C, Sol V, Diab-Assaf M, Simon A and Liagre B. Resistance to 3-HTMC-induced apoptosis through activation of PI3K/

Akt, MEK/ERK, and p38/COX-2/PGE2 pathways in human HT-29 and HCT116 colorectal cancer cells. J Cell Biochem 2016; 117: 2875-2885.

[37] Jubin T, Kadam A, Jariwala M, Bhatt S, Sutariya S, Gani AR, Gautam S and Begum R. The PARP family: insights into functional aspects of poly (ADP-ribose) polymerase-1 in cell growth and survival. Cell Prolif 2016; 49: 421-437.

[38] Ter Brugge P, Kristel P, van der Burg E, Boon U, de Maaker M, Lips E, Mulder L, de Ruiter J, Moutinho C, Gevensleben H, Marangoni E, Majewski I, Jozwiak K, Kloosterman W, van Roosmalen M, Duran K, Hogervorst F, Turner N, Esteller M, Cuppen E, Wesseling J and Jonkers J. Mechanisms of therapy resistance in patient-derived xenograft models of BRCA1-deficient breast cancer. J Natl Cancer Inst 2016; 108.

[39] Yang ZM, Liao XM, Chen Y, Shen YY, Yang XY, Su Y, Sun YM, Gao YL, Ding J, Zhang A, He JX and Miao ZH. Combining 53BP1 with BRCA1 as a biomarker to predict the sensitivity of poly(ADP-ribose) polymerase (PARP) inhibitors. Acta Pharmacol Sin 2017; 38: 1038-1047.

[40] Drean A, Williamson CT, Brough R, Brandsma I, Menon M, Konde A, Garcia-Murillas I, Pemberton HN, Frankum J, Rafiq R, Badham N, Campbell J, Gulati A, Turner NC, Pettitt SJ, Ashworth A and Lord CJ. Modeling therapy resistance in BRCA1/2-mutant cancers. Mol Cancer Ther 2017; 16: 2022-2034.

[41] Lee Y and Rio DC. Mechanisms and regulation of alternative pre-mRNA splicing. Annu Rev Biochem 2015; 84: 291-323.

[42] Naftelberg S, Schor IE, Ast G and Kornblihtt AR. Regulation of alternative splicing through coupling with transcription and chromatin structure. Annu Rev Biochem 2015; 84: 165-198.

[43] Faraoni I, Compagnone M, Lavorgna S, Angelini DF, Cencioni MT, Piras E, Panetta P, Ottone T, Dolci S, Venditti A, Graziani G and Lo-Coco F. BRCA1, PARP1 and γH2AX in acute myeloid leukemia: role as biomarkers of response to the PARP inhibitor olaparib. BBA-Mol Basis Dis 2015; 1852: 462-472.

[44] Park J, Jo YH, Cho CH, Choe W, Kang I, Baik HH and Yoon KS. ATM-deficient human fibroblast cells are resistant to low levels of DNA double-strand break induced apoptosis and subsequently undergo drug-induced premature senescence. Biochem Bioph Res Co 2013; 430: 429-435.

[45] Grewenig A, Schuler N and Rube CE. Persistent DNA damage in spermatogonial stem cells after fractionated low-dose irradiation of testicular tissue. Int J Radiat Oncol 2015; 92: 1123-1131.

[46] Roos WP, Thomas AD and Kaina B. DNA damage and the balance between survival and death in cancer biology. Nat Rev Cancer 2016; 16: 20-33.

[47] Fulda S. Tumor resistance to apoptosis. Int J Cancer 2009; 124: 511-515.

[48] Lin Y, Tang X, Zhu Y, Shu T and Han X. Identification of PARP-1 as one of the transcription factors binding to the repressor element in the promoter region of COX-2. Arch Biochem Biophys 2011; 505: 123-129.

[49] Kalle AM, Sachchidanand S and Pallu R. Bcr-abl-independent mechanism of resistance to imatinib in K562 cells: induction of cyclooxygenase-2 (COX-2) by histone deacetylases (HDACs). Leukemia Res 2010; 34: 1132-1138.

[50] Saikawa Y, Sugiura T, Toriumi F, Kubota T, Suganuma K, Isshiki S, Otani Y, Kumai K and Kitajima M. Cyclooxygenase-2 gene induction causes CDDP resistance in colon cancer cell line, HCT-15. Anticancer Res 2004; 24: 2723-2728.

[51] Yang Lu, Chunmei Shi SQ and Fan Z. Identification and validation of COX-2 as a co-target for overcoming cetuximab resistance in colorectal cancer cells. Oncotarget 2016; 7: 64766-64777.

[52] Hassan L, Pinon A, Limami Y, Seeman J, Fidanzi-Dugas C, Martin F, Badran B, Simon A and Liagre B. Resistance to ursolic acid-induced apoptosis through involvement of melanogenesis and COX-2/PGE2 pathways in human M4Beu melanoma cancer cells. Exp Cell Res 2016; 345: 60-69.

[53] Lin MT, Lee RC, Yang PC, Ho FM and Kuo ML. Cyclooxygenase-2 inducing Mcl-1-dependent survival mechanism in human lung adenocarcinoma CL1.0 cells. Involvement of phosphatidylinositol 3-kinase/Akt pathway. J Biol Chem 2001; 276: 48997-49002.

[54] Xia S, Zhao Y, Yu S and Zhang M. Activated PI3K/Akt/COX-2 pathway induces resistance to radiation in human cervical cancer HeLa cells. Cancer Biother Radiopharm 2010; 25: 317-323.

[55] Dynek JN and Vucic D. Antagonists of IAP proteins as cancer therapeutics. Cancer Lett 2013; 332: 206-214.

[56] Schiewer MJ and Knudsen KE. Transcriptional roles of PARP1 in cancer. Mol Cancer Res 2014; 12: 1069-1080.

[57] Tian YN, Chen HD, Tian CQ, Wang YQ and Miao ZH. Polymerase independent repression of FoxO1 transcription by sequence-specific PARP1 binding to FoxO1 promoter. Cell Death Dis 2020; 11: 71.

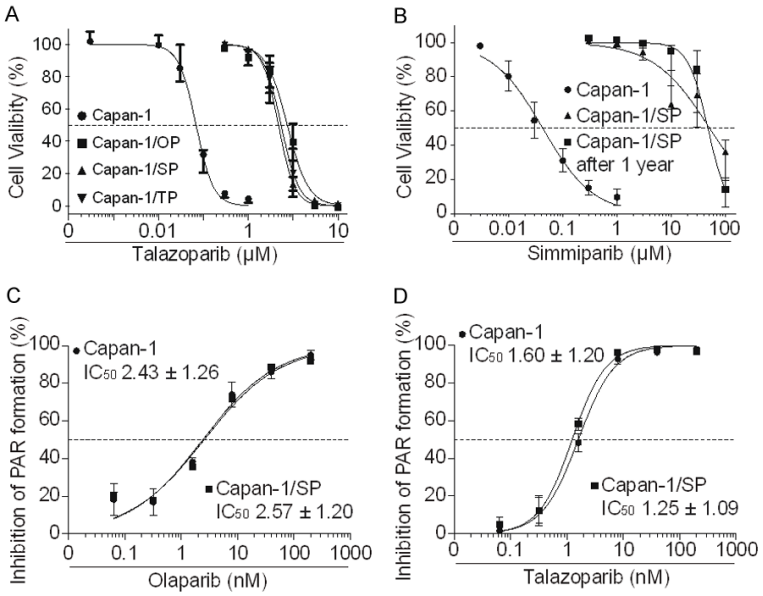

Figure S1. Characteristics of the PAR inhibition in PARPi-resistant variants. (A and B) Cells were treated with simmiparib for 7 days and subjected to SRB assays. (C and D) Inhibitory curves and IC_{50} values of PAR formation inhibited by olaparib (C) and talazoparib (D) Capan-1/SP and Capan-1 cells. Data are presented as the mean ± SD from three independent experiments.

Table S1. Sequence analysis of the full-length sequences of *PTEN*, *BRCA1*, *BRCA2*, *ATM*, and *TP53*

Cell	Gene	Nucleotide changes	Amino acid changes	Gene subregion	heterozygosity	Function change
Capan-1	*BRCA2*	c.6174delT	p.Ser1982Arg fsX22	CDS10	Hom	Frameshift
Capan-1/SP#01	*BRCA2*	c.6174delT	p.Ser1982Arg fsX22	CDS10	Hom	Frameshift
Capan-1/SP#03	*BRCA2*	c.6174delT	p.Ser1982Arg fsX22	CDS10	Hom	Frameshift
Capan-1/OP#01	*BRCA2*	c.6174delT	p.Ser1982Arg fsX22	CDS10	Hom	Frameshift
Capan-1/OP#03	*BRCA2*	c.6174delT	p.Ser1982Arg fsX22	CDS10	Hom	Frameshift
Capan-1/TP#01	*BRCA2*	c.6174delT	p.Ser1982Arg fsX22	CDS10	Hom	Frameshift
Capan-1/TP#02	*BRCA2*	c.6174delT	p.Ser1982Arg fsX22	CDS10	Hom	Frameshift
Capan-1	*BRCA2*	-	-	-	-	-
Capan-1/SP#01	*BRCA2*	c.6841+2T>C	-	Intron 11	Het	Splice
Capan-1/SP#03	*BRCA2*	c.6841+2T>C	-	Intron 11	Het	Splice
Capan-1/OP#01	*BRCA2*	c.6841+2T>C	-	Intron 11	Het	Splice
Capan-1/OP#03	*BRCA2*	c.6841+2T>C	-	Intron 11	Het	Splice
Capan-1/TP#01	*BRCA2*	c.6841+1G>A	-	Intron 11	Het	Splice
Capan-1/TP#02	*BRCA2*	c.6841+1G>A	-	Intron 11	Het	Splice
Capan-1	*TP53*	c.476C>T	p.Ala159Val	CDS4	Hom	Missense
Capan-1/SP#01	*TP53*	c.476C>T	p.Ala159Val	CDS4	Hom	Missense
Capan-1/SP#03	*TP53*	c.476C>T	p.Ala159Val	CDS4	Hom	Missense
Capan-1/OP#01	*TP53*	c.476C>T	p.Ala159Val	CDS4	Hom	Missense
Capan-1/OP#03	*TP53*	c.476C>T	p.Ala159Val	CDS4	Hom	Missense
Capan-1/TP#01	*TP53*	c.476C>T	p.Ala159Val	CDS4	Hom	Missense
Capan-1/TP#02	*TP53*	c.476C>T	p.Ala159Val	CDS4	Hom	Missense
Capan-1	*BRCA1*	c.4837A>G	p.Ser1613Gly	CDS14	Het	Missense
Capan-1/SP#01	*BRCA1*	c.4837A>G	p.Ser1613Gly	CDS14	Het	Missense
Capan-1/SP#03	*BRCA1*	c.4837A>G	p.Ser1613Gly	CDS14	Het	Missense
Capan-1/OP#01	*BRCA1*	c.4837A>G	p.Ser1613Gly	CDS14	Het	Missense
Capan-1/OP#03	*BRCA1*	c.4837A>G	p.Ser1613Gly	CDS14	Het	Missense
Capan-1/TP#01	*BRCA1*	c.4837A>G	p.Ser1613Gly	CDS14	Het	Missense
Capan-1/TP#02	*BRCA1*	c.4837A>G	p.Ser1613Gly	CDS14	Het	Missense
Capan-1	*PTEN*	-	-	-	-	-
Capan-1/SP#01	*PTEN*	-	-	-	-	-
Capan-1/SP#03	*PTEN*	-	-	-	-	-
Capan-1/OP#01	*PTEN*	-	-	-	-	-
Capan-1/OP#03	*PTEN*	-	-	-	-	-
Capan-1/TP#01	*PTEN*	-	-	-	-	-
Capan-1/TP#02	*PTEN*	-	-	-	-	-
Capan-1	*ATM*	c.5557G>A	p.Asp1853Asn	CDS36	Het	Missense
Capan-1/SP#01	*ATM*	c.5557G>A	p.Asp1853Asn	CDS36	Het	Missense
Capan-1/SP#03	*ATM*	c.5557G>A	p.Asp1853Asn	CDS36	Het	Missense
Capan-1/OP#01	*ATM*	c.5557G>A	p.Asp1853Asn	CDS36	Het	Missense
Capan-1/OP#03	*ATM*	c.5557G>A	p.Asp1853Asn	CDS36	Het	Missense
Capan-1/TP#01	*ATM*	c.5557G>A	p.Asp1853Asn	CDS36	Het	Missense
Capan-1/TP#02	*ATM*	c.5557G>A	p.Asp1853Asn	CDS36	Het	Missense

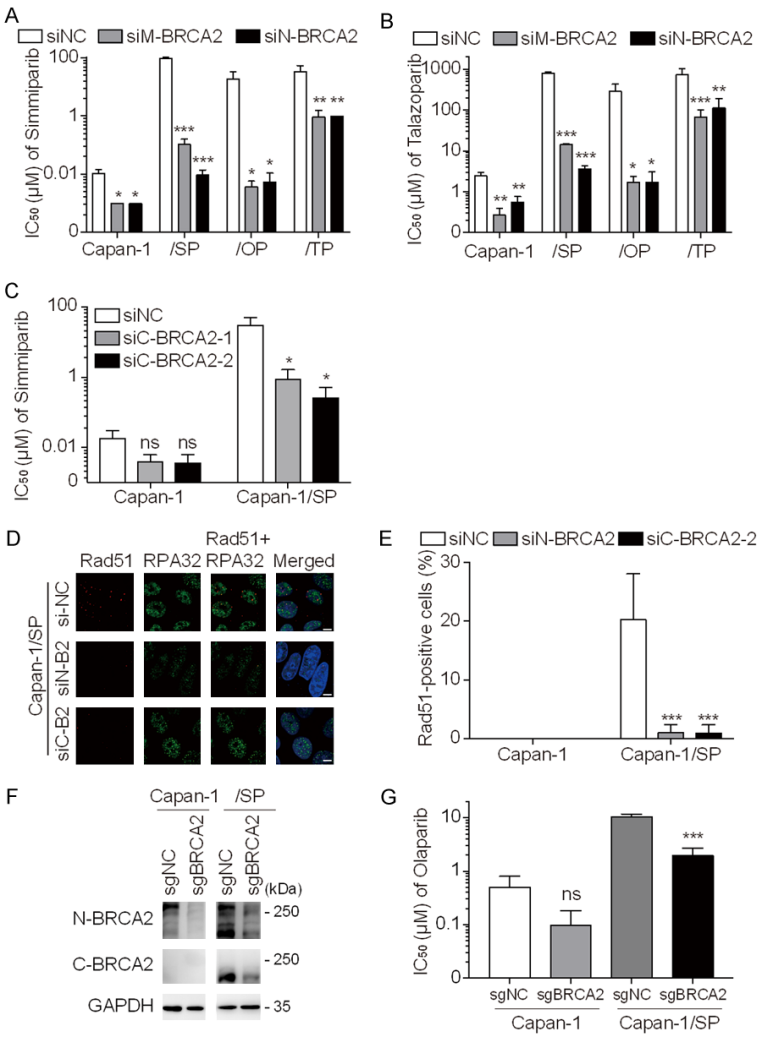

Figure S2. Knockdown or genetic depletion of BRCA2 partially restores the sensitivity of PARPi-resistant variants to PARPi. (A and B) BRCA2 silencing by siM-BRCA2 and siN-BRCA2 partially restored simmiparib (A) and talazoparib (B) sensitivity. (C) Depletion of the novel BRCA2 isoform partially restored simmiparib sensitivity. (D and E) the foci formation of Rad51 was reduced in Capan-1/SP-siBRCA2 (siN-B2 equal siN-BRCA2, siC-B2 equal siC-BRCA2-2) cells exposed to irradiated (6 Gy) and fixed 6 h after ionizing radiation and then detected by confocal microscopy. Representative images (D), and quantitative data (E). Scale bar: 5 μm. Cells that contained three or more Rad51 per nucleus were considered as Rad51-positive cells. At least 200 cells were analyzed in each group. (F) Depletion of BRCA2 by CRISPR/Cas9 in Capan-1/SP and Capan-1 cells was confirmed by western blotting. (G) Depletion of BRCA2 partially restored olaparib sensitivity. Cells were treated with olaparib for 7 days and then subjected to SRB assays. Data are presented as the mean ± SD from three independent experiments. *P<0.05; **P<0.01; ***P<0.01.

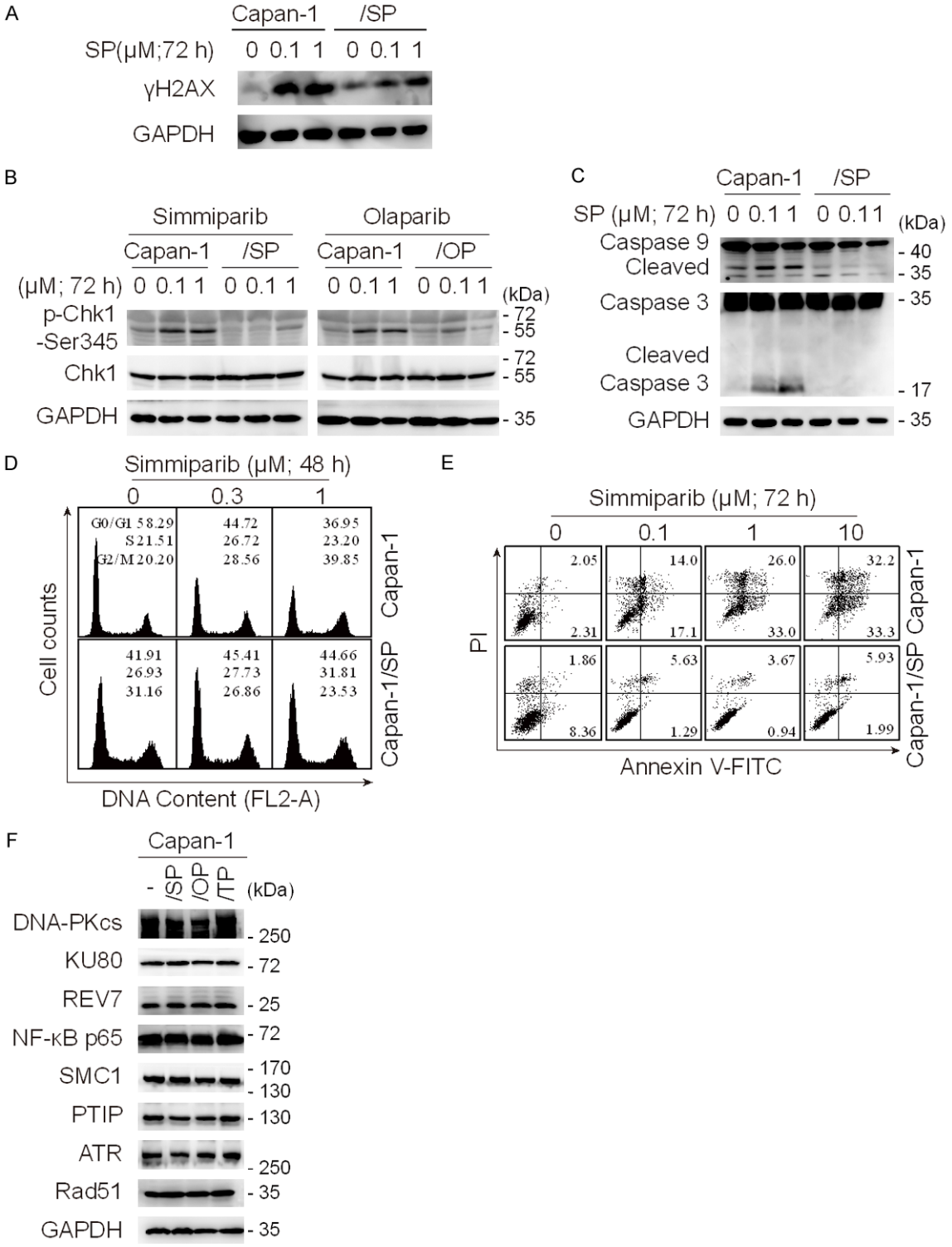

Figure S3. Characteristics of the DNA-damage checkpoint, cell cycle distribution, and apoptosis in PARPi-resistant variants. (A-C) Cells were treated with PARPi for 72 h, and then subjected to Western blotting for γH2AX(A), p-Chk1 (B) and caspase 3/9 cleaved (C). (D and E) G2/M arrest (D) and apoptosis (E) induced by simmiparib (SP) was determined by flow cytometry in Capan-1/SP and Capan-1 cells. (F) Protein levels of DNA repair proteins detected by Western blotting in PARPi-resistant variants and Capan-1 cells.

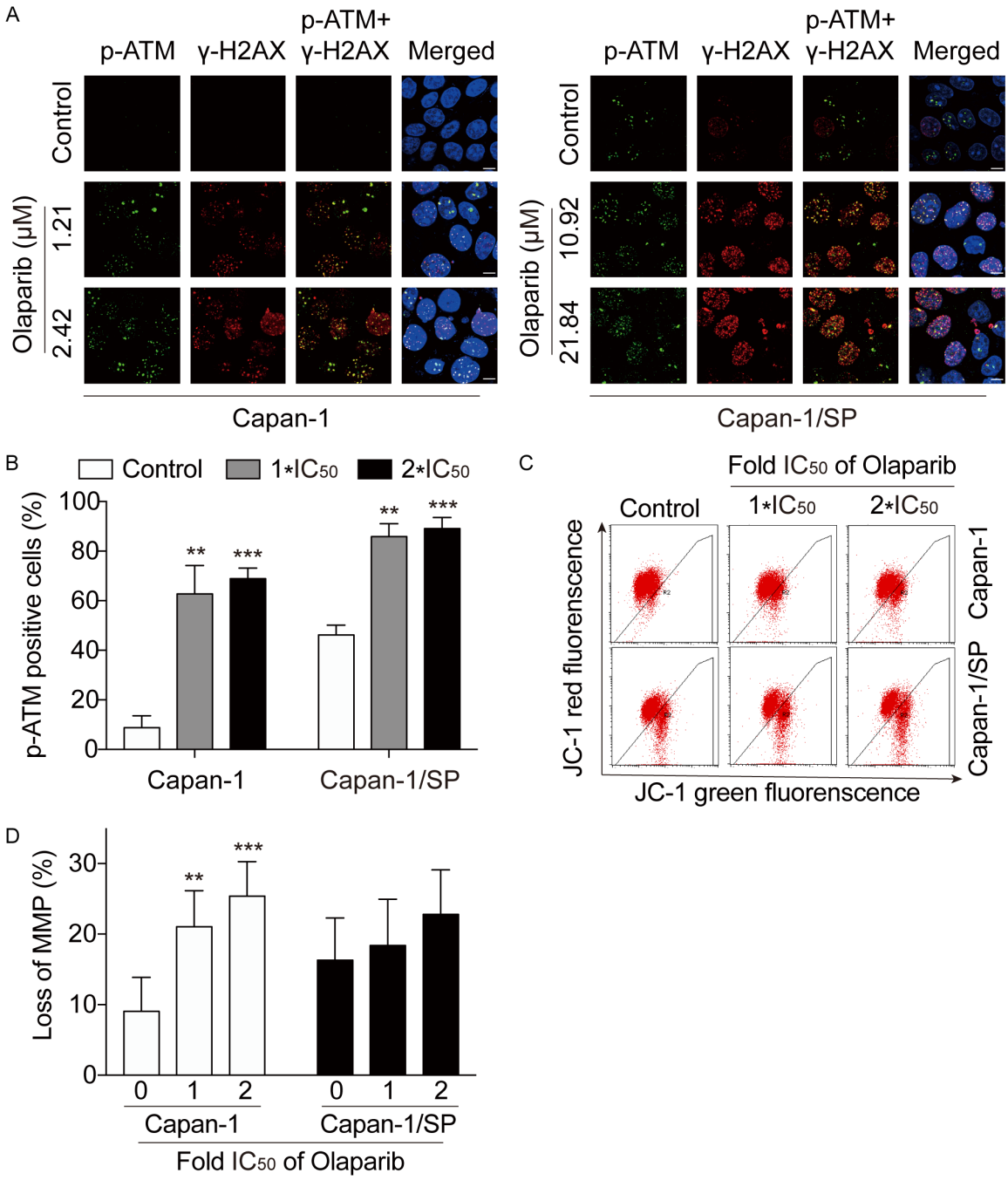

Figure S4. Apoptosis signals triggered by PARPi are almost completely abrogated in the resistant cells. (A and B) DNA damage accumulation was similar in parental and resistant cells. Cells that contained three or more p-ATM or γH2AX foci per nucleus were considered p-ATM- or γH2AX-positive cells. At least 500 cells were analyzed in each group. Representative images are presented in (A) and Data are presented as the mean ± SD from three independent experiments in (B). **P<0.01; ***P<0.01. (C and D) Capan-1/SP and Capan-1 cells were treated with olaparib for 72 h, after which loss of the MMP was analyzed by flow cytometry. Representative images are presented in (C) and the data from eight independent experiments are presented as the mean ± SD in (D). **P<0.01; ***P<0.001.

Table S2. RNA-Seq analysis revealed significantly changed expression of apoptotic-related genes

Number	GeneSymbol	Capan-1/OP logFC	Capan-1/SP logFC	Number	GeneSymbol	Capan-1/OP logFC	Capan-1/SP logFC
1	C8orf4	8.67119973	6.34007946	20	BIRC3	3.18848667	2.53976708
2	CCL2	7.3801593	8.06208195	21	RAG1	3.15924835	3.69354776
3	S100A9	6.96982487	4.70832958	22	FAM3B	3.14862168	2.95635614
4	CD74	6.20152693	3.02632197	23	TGM2	3.14707622	3.13123618
5	XDH	5.4780187	4.61886523	24	MEIS3	3.14058891	3.66545116
6	CD40	5.46523938	4.90039259	25	PNMA2	3.06575162	2.93463579
7	PTGS2/COX-2	5.31852361	4.54395214	26	ANGPT1	3.01090861	4.58405441
8	ANGPTL4	4.26991154	2.47176894	27	PRKCQ	2.85623179	3.66038871
9	NKX3-2	4.10245607	4.38643162	28	ZC3H12A	2.8527399	2.74651
10	VNN1	4.04710727	4.30092591	29	ADAMTSL4	2.74472207	3.46029737
11	ITGB2	4.01454589	2.72805418	30	RPS6KA2	2.72959674	4.6416808
12	NOD2	3.80267656	4.60463131	31	H1F0	2.37207868	2.35853867
13	SGK1	3.75379542	4.15928223	32	LGALS1	2.35083066	3.1223118
14	LCN2	3.64564842	2.39242894	33	SMO	2.32037672	2.64962465
15	NFATC4	3.64299656	2.45288506	34	TNFSF9	2.2412297	3.4284267
16	IGFBP3	3.63673407	4.68700318	35	ADAM8	2.21738405	3.51488591
17	KCNIP3	3.43696737	3.20034259	36	NFKBIA	2.15052187	2.6423121
18	TNFAIP3	3.35226266	4.04392761	37	EPHA7	-5.566474017	-2.631839336
19	TNFSF12	3.28172862	2.69191197	38	ROBO2	-3.280592355	-8.634681447

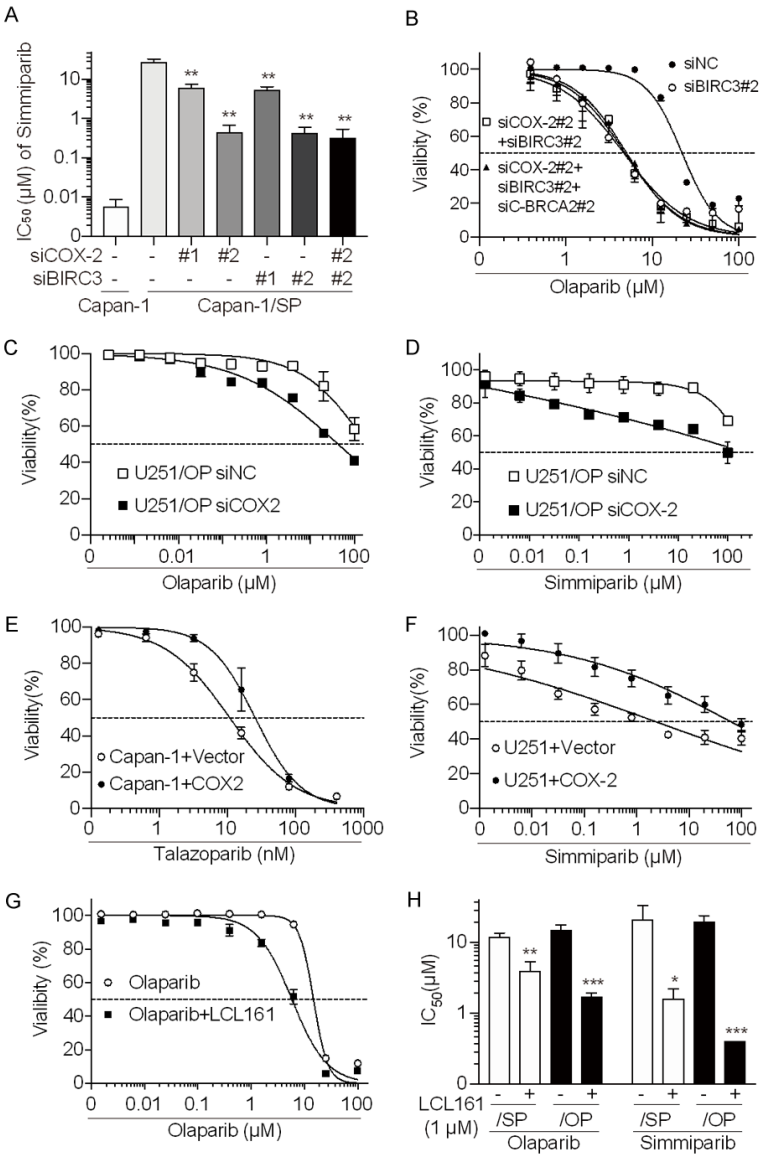

Figure S5. Depletion of COX-2 or BIRC3 or combination with BIRC3 inhibitor LCL161 partially restores the sensitivity of PARPi-resistant variants to PARPi. (A) After transfection with the indicated siRNA, cells were treated with simmiparib for 7 days and then subjected to SRB assays. (B) Knockdown of BIRC3 or COX-2/BIRC3 or COX-2/BIRC3/C-BRCA2 re-sensitized Capan1-/SP cells to olaparib. After transfection with the indicated siRNA, cells were treated with olaparib for 7 days and then subjected to SRB assays. (C and D) Knockdown of COX-2 re-sensitized U251/OP cells to olaparib (C) and simmiparib (D). U251/OP cells were transfected with siCOX-2 for 24 h, then treated with PARPi for 7 days and assessed by SRB assays. (E and F) Exogenous expression of COX-2 reduced the sensitivity of PARPi in U251 cells. U251 cells were infected with lentiviral (MOI = 5) of COX-2 or control vector for 48 h, and confirmed by Western blotting. Cells were treated with talazoparib (E) and simmiparib (F) for 7 days and subjected to SRB assays. (G and H) Capan-1/SP cells were treated with olaparib alone or in combination with 1 μM LCL161 for the indicated time, and then the cell viability (IC_{50} values) was assessed by SRB assays. All of the data are presented as the mean ± SD from three independent experiments. *P<0.05; **P<0.01; ***P<0.001.

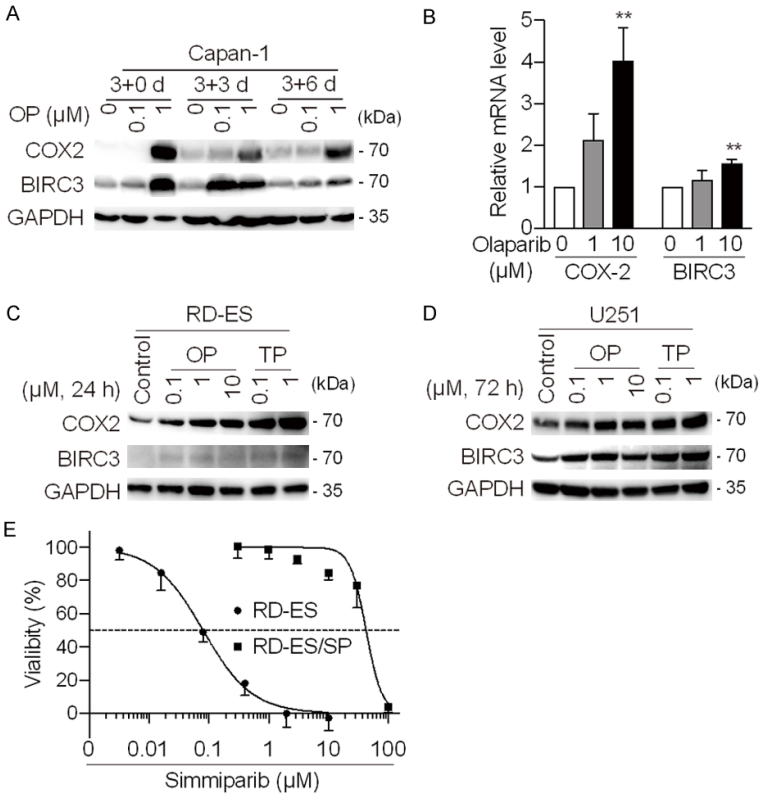

Figure S6. COX-2/BIRC3 overexpression was observed in PARPi treatment cells or PARPi-resistant variants. (A) Protein levels of COX-2 and BIRC3 were detected by western blotting after 3-day olaparib (OP) treatment, and 3 days or 6 days after washing off olaparib in Capan-1 cells. (B) Relative mRNA levels of COX-2 and BIRC3 were determined by qPCR in RD-ES cells. (C and D) Protein levels of COX-2 and BIRC3 were detected by western blotting after olaparib (OP) and talazoparib (TP) treatment in RE-ES cells for 24 h (C) and U251 cells for 72 h (D). (E) PARPi-resistant variants of RD-ES resistant to PARPi simmiparib, cells were treated with simmiparib for 3 days and then subjected to CCK-8 assays. Data are presented as the mean ± SD from three independent experiments. *P<0.05; **P<0.01; ***P<0.001.